Geochronology of high-grade metamorphism in the Sveconorwegian belt, S. Norway: U-Pb, Th-Pb and Re-Os data

Bernard Bingen, William J. Davis, Michael A. Hamilton, Ane K. Engvik, Holly J. Stein, Øyvind Skår & Øystein Nordgulen

Bingen, B., Davis, W.J., Hamilton, M.A., Engvik, A., Stein, H.J., Skår, Ø. & Nordgulen, Ø.: geochronology of high-grade metamorphism in the Sveconorwegian belt, S. Norway: U-Pb, Th-Pb and Re-Os data. *Norwegian Journal of Geology* vol. 88, pp 13-42. Trondheim 2008. ISSN 029-196X.

The timing of Sveconorwegian high-grade metamorphism is evaluated in the four lithotectonic units / terranes exposed in the Sveconorwegian belt in South Norway. U-Pb, Th-Pb and Re-Os data were obtained from 21 samples of Mesoproterozoic ortho- and paragneisses. In the Bamble Terrane, SIMS monazite U-Pb data constrain peak amphibolite- to granulite-facies metamorphism between 1137 ±1 and 1127 ±6 Ma, and unroofing at 1107 ±9 Ma. In the Kongsberg Terrane, a molybdenite Re-Os date at 1112 ±4 Ma and a monazite U-Pb date at 1092 ±1 Ma bracket amphibolite-facies metamorphism. In the Idefjorden Terrane, west of the Oslo rift, a pulse of Gothian metamorphism at 1539 ±8 Ma and three pulses of Sveconorwegian metamorphism at 1091 ±18 Ma, 1052 ±4 to 1043 ±8 Ma and 1024 ±9 Ma are recorded by monazite, zircon and titanite data. Amphibolite-facies metamorphism peaked at 1052 ±4 Ma in the kyanite field (1.00-1.17 GPa, 688-780 °C). At the boundary between the Idefjorden and Telemarkia Terranes, SIMS zircon U-Pb data constrain amphibolite-facies metamorphism between 1012 ±7 and 1008 ±14 Ma and provide a maximum age for shearing along the Vardefjell Shear Zone between these two terranes. Amphibolite-facies metamorphism in the Telemarkia hanging wall of the Vardefjell Shear Zone is coeval at 1014 ±1 Ma. In the Suldal Sector of the Telemarkia Terrane, monazite data yield an age of 1005 ±7 Ma for amphibolite-facies migmatitization. In the Rogaland-Vest Agder Sector of the Telemarkia Terrane, paired U-Pb and Th-Pb ID-TIMS monazite analyses date monazite growth to have been between 1013 ±5 and 980 ±5 Ma during M1 intermediate-pressure regional metamorphism, and between 927 ±5 and 922 ±5 Ma during M2 low-pressure high- to ultrahigh-temperature metamorphism. SIMS monazite dates at 1032 ±5 and 990 ±8 Ma in a granulite, situated outside the area affected by M2 metamorphism, demonstrate granulite-facies conditions during M1 metamorphism. Available data show that the four terranes in South Norway have distinct metamorphic histories. The Bamble and Kongsberg Terranes show evidence for early-Sveconorwegian metamorphism between 1140 and 1080 Ma. The Idefjorden Terrane, though locally affected by this early metamorphism, was mainly reworked by medium to high-pressure metamorphism between 1050 and 1025 Ma. The Telemarkia Terrane was reworked later between c. 1035 and 970 Ma. A high-temperature metamorphic phase at 930-920 Ma is specific for the Telemarkia Terrane and is related to post-collisional intrusion of the Rogaland anorthosite-mangerite-charnockite (AMC) Complex.

Bernard Bingen, Holly J. Stein, Ane K. Engvik, Øyvind Skår & Øystein Nordgulen Geological Survey of Norway, 7491 Trondheim, Norway (bernard.bingen@ngu.no). William J. Davis, Geological Survey of Canada, K1A 0E8 Ottawa, Canada. Michael A. Hamilton, Department of Geology, University of Toronto, M5S3B1 Toronto, Canada. Holly J. Stein, AIRIE Program, Department of Geosciences, Colorado State University, CO80523-1482 Fort Collins, USA

Introduction

The Mesoproterozoic crust in the southwest part of the Fennoscandian Shield was reworked during the Sveconorwegian orogeny (Pasteels & Michot 1975; Berthelsen 1980; Demaiffe & Michot 1985; Falkum 1985). Though this idea has been well established in the literature for decades, it is not until recently that the Sveconorwegian age of high-grade metamorphism was established in all lithotectonic units of the Sveconorwegian orogenic belt. Especially controversial was the timing of granulite-facies metamorphism in the Bamble Terrane in south Norway (Kullerud & Dahlgren 1993) and the Eastern Segment in southwestern Sweden (Johansson et al. 1991). Today, the objective is to improve the chronologic and tectonic model for the Sveconorwegian orogenic event itself. In this paper, monazite, zircon and titanite U-Pb data and molybdenite Re-Os data are reported from metamorphic rocks to date high-grade metamorphism in the four main lithotectonic units in south Norway. A pressure-temperature estimate is reported for one critical sample. These data were derived from material collected over several years, in the course of regional geologic investigations, and analysed using different analytical methods. Together, they provide a significantly enlarged field coverage, and point to important differences in the metamorphic evolution of the four lithotectonic units. These data are integrated in an orogen-scale tectono-metamorphic model in a companion paper (Bingen et al. 2008).

Geological setting

The Sveconorwegian Belt (Berthelsen 1980) south of the Caledonian front is divided into five main lithotectonic units separated by crustal scale shear zones (Fig. 1). The easternmost unit, traditionally called the Eastern Seg-

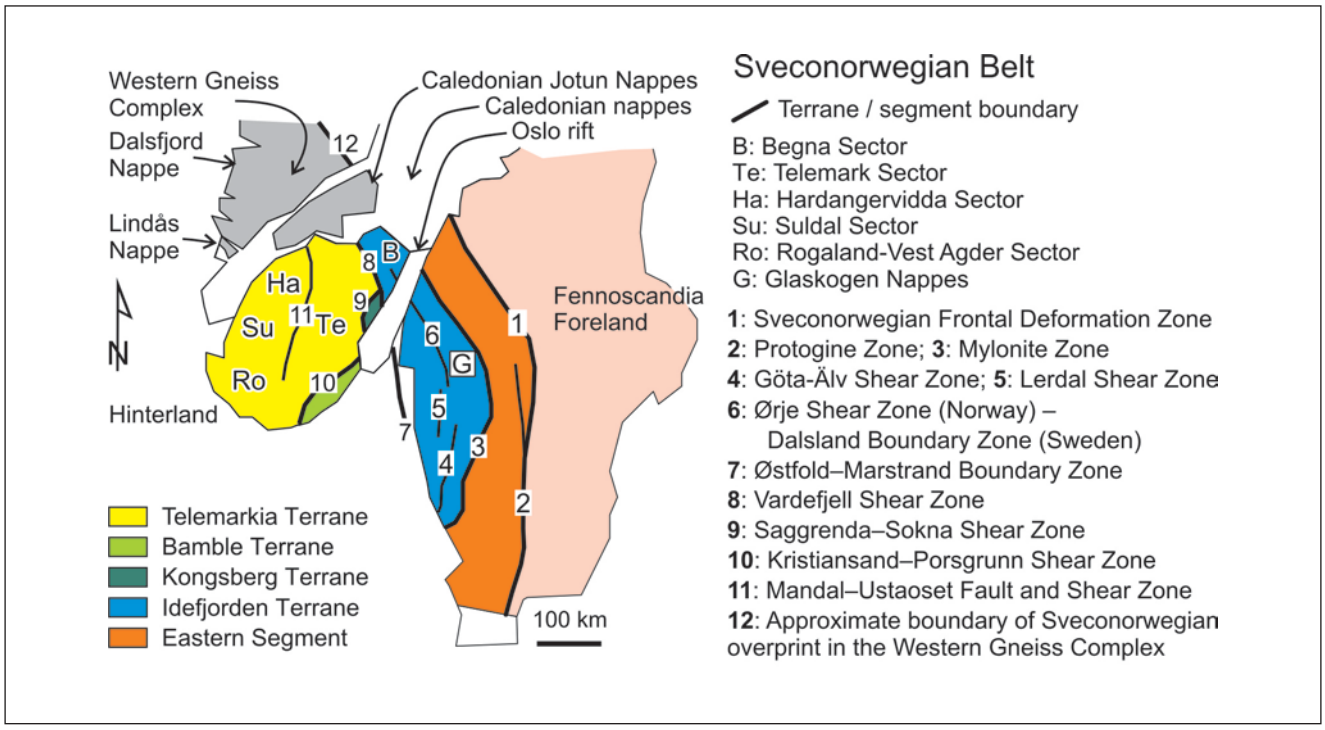

Fig. 1. Situation map of SW Scandinavia showing the main lithotectonic units and shear zones of the Sveconorwegian orogenic belt.

ment, is regarded as a parautochthonous unit directly linked to the Fennoscandia foreland (Söderlund et al. 1999). The other lithotectonic units were tectonically transported (with respect to Fennoscandia) during the Sveconorwegian orogeny and are referred to as terranes in this paper. These are the Idefjorden, Kongsberg, Bamble and Telemarkia Terranes (Fig. 1; Bingen et al. 2005). The samples analysed in this study were collected in these four terranes.

Idefjorden Terrane

The Idefjorden Terrane (Fig. 1) is made up of 1660-1520 Ma plutonic and volcanic rocks, associated with greywacke-bearing metasedimentary sequences (Brewer et al. 1998; Bingen et al. 2001b; Andersen et al. 2004a; Åhäll & Connelly 2008). These lithologies were assembled during the Gothian accretionary event (Andersen et al. 2004a; Åhäll & Connelly 2008). The Idefjorden Terrane hosts a 1340-1250 Ma bimodal metaplutonic suite (Austin Hegardt et al. 2007) and 960-920 Ma post-collisional norite-granite plutons (Hellström et al. 2004).

The Idefjorden Terrane displays a general N-S to NW-SE Sveconorwegian structural grain. It contains several amphibolite-facies orogen-parallel shear zones, including the Göta Älv Shear Zone (Park et al. 1991), as well as a nappe complex, the Glaskogen Nappes (Lindh et al. 1998; Fig. 1). Sveconorwegian metamorphism ranges from greenschist- to amphibolite-facies, locally to granulite-facies conditions.

Bamble and Kongsberg Terranes

The Bamble and Kongsberg Terranes are two small terranes, made up of 1570-1460 Ma plutonic suites associated with quartzite or greywacke-dominated metasediment complexes (Starmer 1985; Starmer 1991; Andersen et al. 2004a). The Bamble Terrane contains 1200-1180 Ma gabbro-tonalite metaplutons (Tromøy complex), 1170-1150 Ma granite-charnockite metaplutons, and 990-920 Ma post-collisional granite plutons (Kullerud & Dahlgren 1993; Knudsen & Andersen 1999; Andersen et al. 2001; Andersen et al. 2004a).

The Kongsberg Terrane shows a steep N-S trending Sveconorwegian amphibolite-facies structural grain (Starmer 1985; Andersen & Munz 1995). Peak P-T conditions are in the sillimanite stability field. Post-peak kyanite-bearing assemblages are recorded in talc-kyanite schist units (Munz 1990). The Bamble Terrane has a pronounced NE–SW trending structural grain defined by a strong planar fabric, banding and attenuation of lithological units (Starmer 1985; Starmer 1991; Kullerud & Dahlgren 1993). Regional metamorphic grade increases across strike to the southeast and reaches intermediate-pressure granulite-facies in the Arendal area (Touret 1971; Smalley et al. 1983; Nijland & Maijer 1993; Knudsen & Andersen 1999). Four main isograds are mapped. These are, from northwest to southeast, muscovite-out in pelitic gneiss, cordierite-in in pelitic gneiss, and orthopyroxene-in successively in amphibolite and felsic gneiss (Nijland & Maijer 1993). Peak pressure-temperature conditions are estimated at 0.70 ±0.11 GPa and 793 ±58 °C in the core of the granulite-facies domain, using garnet-pyroxene thermobarometry (Harlov 2000). These

values are in the sillimanite stability field in accordance with petrographic observations. Pre-peak and post-peak kyanite are reported in the amphibolite-facies domain (Visser & Senior 1990; Nijland & Maijer 1993).

Telemarkia Terrane

The Telemarkia Terrane (Fig. 1, 2) is characterized by 1520-1480 Ma volcanic and plutonic suites, associated with and overlain by quartzite-bearing metasedimentary sequences (Dons 1960; Bingen et al. 2001b; Laajoki et al. 2002; Bingen et al. 2005). It contains several pre-Sveconorwegian deformed magmatic suites at 1280-1260 Ma and 1220-1130 Ma (Heaman & Smalley 1994; Laajoki et al. 2002; Bingen et al. 2002; Andersen et al. 2004b; Andersen et al. 2007) and several Sveconorwegian plutonic suites (Fig. 2). These include 1050-1000 Ma syn-collisional granitoids, 970-930 Ma post-collisional granitoid plutons, and the 930-920 Ma Rogaland anorthosite-mangerite-charnockite (AMC) Complex (Fig. 2) (Schärer et al. 1996; Bingen & van Breemen 1998b; Andersen et al. 2001; Bogaerts et al. 2003; Bolle et al. 2003; Vander Auwera et al. 2003).

For descriptive purposes, the Telemarkia Terrane is divided into four "sectors": the Telemark, Hardangervidda, Suldal and Rogaland-Vest Agder Sectors (Bingen et al. 2005). The Hardangervidda Sector consists of amphibolite-facies gneisses with a general E-W structural grain (Sigmond 1998). The Telemark and Suldal Sectors are characterized by greenschist- to epidote-amphibolite-facies supracrustal sequences, associated with plutonic rocks. In the central part of the Telemark Sector, the Telemark supracrustal rocks show well-preserved volcanic and sedimentary textures and an extensive record of their original stratigraphic relationships. In the south of the Telemark Sector, supracrustal rocks abut a NE-SW to N-S trending amphibolite-facies gneiss complex. This gneiss complex forms the foot wall of the Kristiansand-Porsgrunn Shear Zone, and is referred to as the South Telemark Gneisses by Andersen et al. (2007).

The Rogaland-Vest Agder Sector corresponds to the southwesternmost amphibolite- to granulite-facies gneiss domain. Four isograds reflect an increase of metamorphic grade towards the Rogaland AMC complex (Fig. 2; Tobi et al. 1985). The isograds are, towards the southwest, clinopyroxene-in in granodioritic gneiss, orthopyroxene-in in granitic gneiss, osumilite-in in paragneiss, and pigeonite-in in granitic gneiss. Osumilite assemblages are indicative of high- to ultra-high temperature, low-pressure and water-poor granulite-facies conditions (Holland et al. 1996). Formation of the pigeonite isograd requires temperatures exceeding 865 °C. Westphal et al. (2003) estimate that peak temperatures increase

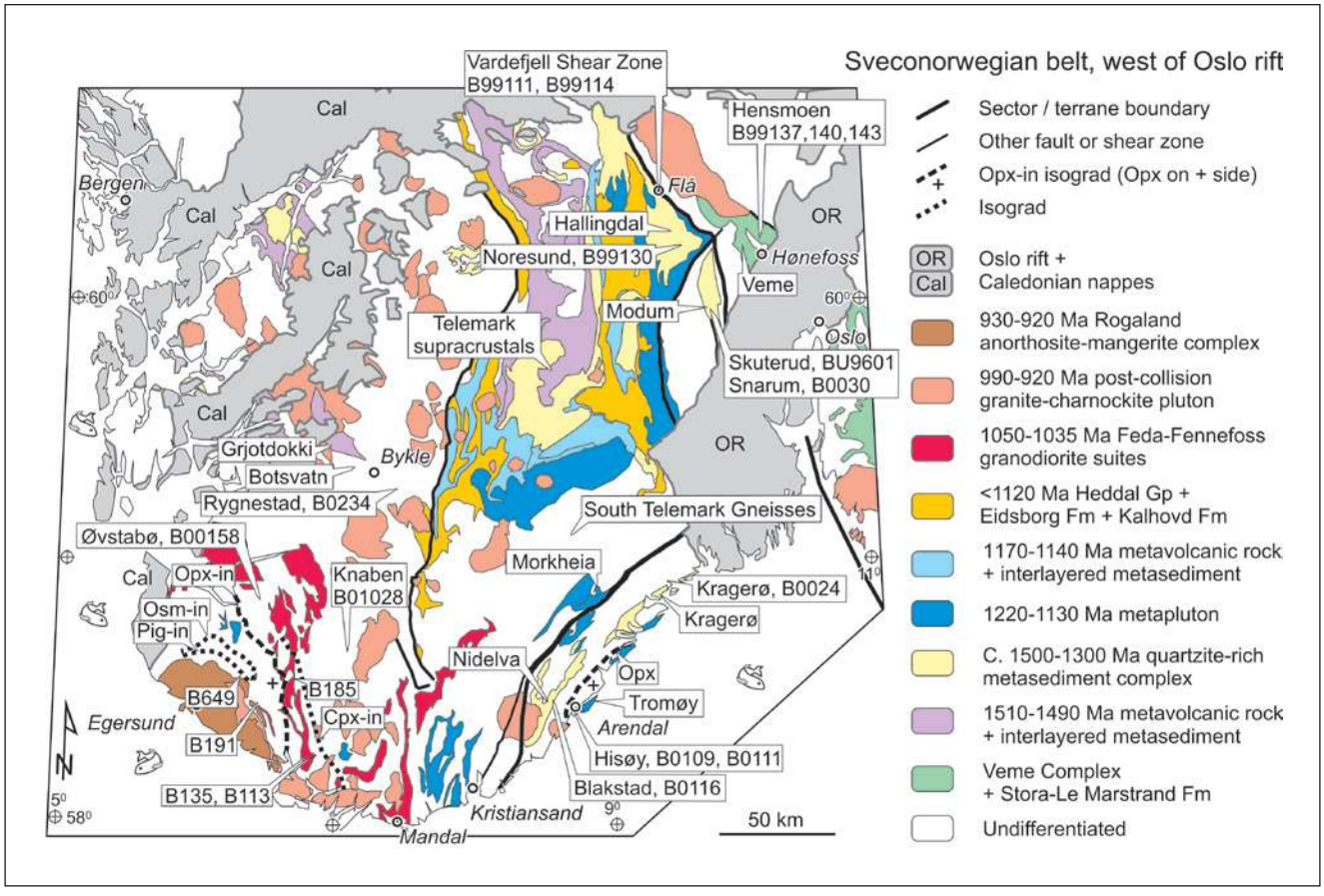

Fig. 2. Simplified geologic map of the Sveconorwegian belt, west of the Oslo rift, showing the location of granulite-facies domains, of supracrustal sequences and gneiss complexes cited in the text, main post-1220 Ma magmatic suites, and samples analysed in this study.

towards the contact of the AMC complex, from c. 760 °C 13 km from the contact to more than 900 °C 5 km from the contact and at a pressure of 0.5 GPa. The close parallelism between the osumilite and pigeonite isograds and the contact of the Rogaland AMC complex is good evidence for a relation between high-temperature metamorphism and intrusion of the magmatic complex (Tobi et al. 1985). In the Rogaland-Vest Agder Sector, there is petrological evidence for three metamorphic phases (M1 to M3) (Tobi et al. 1985). High- to ultrahigh-temperature granulite-facies assemblages (M2) commonly include relics of older high-grade medium-pressure assemblages (M1), and they are themselves commonly surrounded by post-peak corona textures (M3). Orthopyroxene-bearing assemblages are reported for both M1 and M2, suggesting superposition of two granulite-facies events, one related to regional metamorphism (M1) and the other related to intrusion of the anorthosite complex (M2) (Tobi et al. 1985; Vander Auwera 1993; Westphal et al. 2003).

Methods

Analytical methods

U-Pb geochronological data were collected on zircon, titanite and monazite from 20 samples (Table 1). Standard methods of mineral separation were used, including water-table, magnetic, and heavy liquid separation. Crystals were selected for analysis by hand picking under alcohol. For Secondary Ion Mass Spectrometry (SIMS) and laser ablation - inductively coupled plasma mass spectrometry (LA-ICPMS) analyses, selected crystals were mounted in epoxy, and polished to approximately the middle of the grains. Cathodoluminescence (CL) images of zircon and backscattered electron (BSE) images of monazite were taken with a scanning electron microscope before analysis (Fig. 3).

SIMS U-Pb analyses were performed with the SHRIMP II instrument at the Geological Survey of Canada on zircon (Table 2) and monazite (Table 3) following procedures outlined by Stern (1997), Stern and Berman (2000) and Stern and Amelin (2003). The samples were analysed in Kohler illumination mode, with primary beam diameters of c. 15, 20 and 30 µm. Zircon analyses were calibrated relative to the in-house standard BR266 with an age of 559 Ma. Monazite Th-Pb and U-Pb analyses were calibrated relative to the in-house standard 2908 with an age of 1795 Ma. Common Pb detected in the analyses is mainly attributed to contamination at the surface of the sample. Consequently, a common Pb correction was applied using the ^{204}Pb concentration and present-day isotopic composition (Stacey & Kramers 1975). As discussed in Stern and Berman (2000), an unidentified isobar complicates the determination of ^{204}Pb in monazite with a high Th content. A significant interference was detected for one of the samples (B0024), that could not be resolved by applying an energy offset to the secondary ion beam. For this sample, the age is thus reported without common Pb correction, and is thus slightly overestimated by a maximum of 10 m.y. and probably less than 5 m.y.

Paired Th-Pb, U-Pb analyses of non-abraded single-grain fractions of monazite were performed by isotope dilution-thermal ionisation mass spectrometry (ID–TIMS)

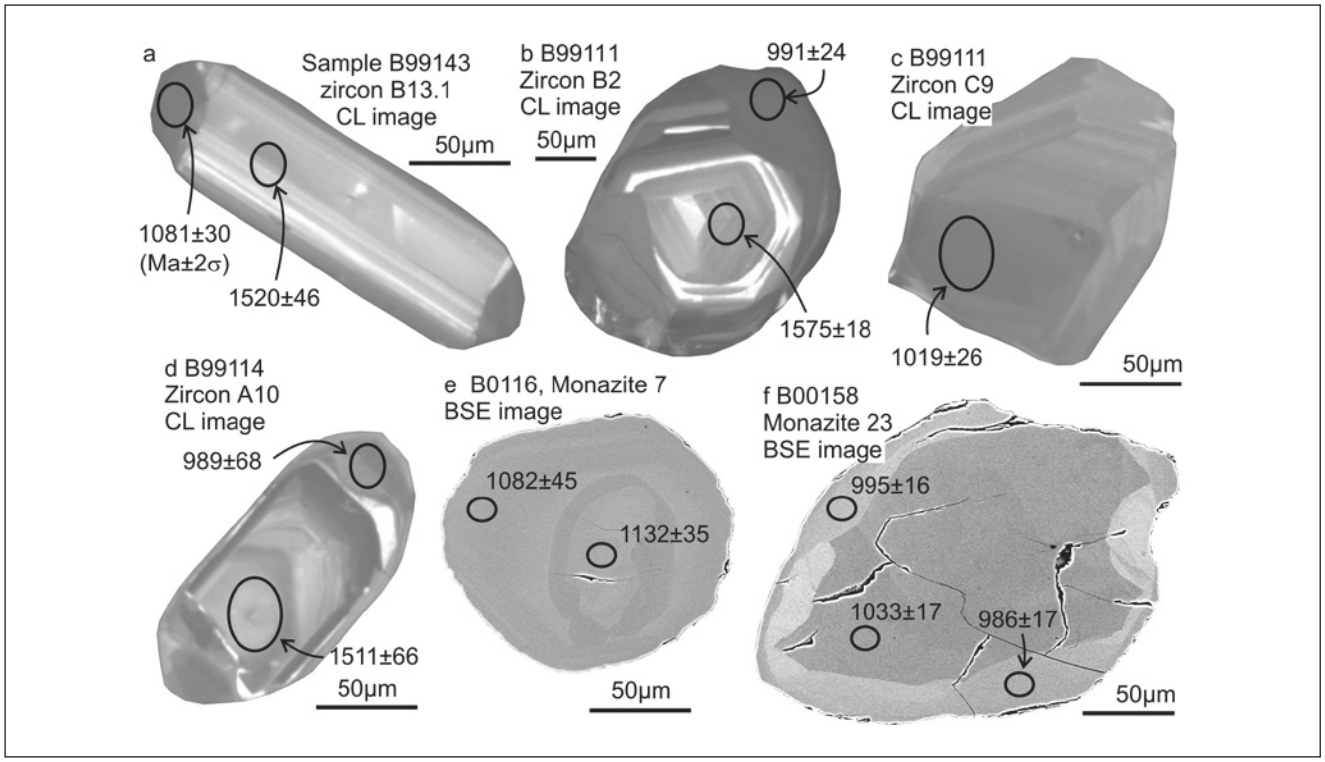

Fig. 3. Cathodoluminescence (CL) images of zircon and backscattered electron images (BSE) of monazite, with location of ion microprobe analyses.

Table 1. Sample location and summary of geochronological data

Sample	Locality	Lithology	x (1)	y (1)	Rock forming minerals (2)	Accessory minerals	Selected age (Ma)	Interpretation	Method (3)	Fig. (4)
Bamble Terrane										
B0109	Hisøy	Metapelite	486696	6476115	Qtz, Grt, Kfs, Pl, Bt, Sil	Opaque, Mnz, Ap, Zrn	Mnz: 1137±1	Metamorphism	U-Pb ID-TIMS	4a-c
B0111	Hisøy	Metapelite	486285	6476162	Qtz, Grt, Kfs, Pl, Bt, Sil	Opaque, Gr, Rt, Mnz, Ap, Zrn	Mnz: 1135±6	Metamorphism	U-Pb SIMS	4d
B0024	Kragerø	Quartzite	532147	6532648	Qtz, Bt, Sil, Trm, Ms	Mnz, Xnt, Zrn, Ap?	Mnz: 1127±6	Metamorphism	U-Pb SIMS	4f
B0116	Blakstad	Quartzite	479326	6483907	Qtz, Bt, Ms, Pl	Mnz, Zrn, Ap	Mnz: 1134±14, 1107±9	Metamorphism	U-Pb SIMS	4e
Kongsberg Terrane										
BU9601	Skuterud	Sulfide ore	548220	6648750			Moly: 1112±4	Metamorphism	Re-Os ID-NTIMS	
B0030	Snarum	Nodular gneiss	545343	6654001	Qtz, Bt, Sil, Trm, Ms	Mnz, Xnt, Zrn, Ap?	Mnz: 1092±1	Metamorphism	U-Pb ID-TIMS	5a-c
Idefjorden Terrane										
B99137	Hensmoen	Metapelite	569100	6677300	Qtz, Kfs, Pl, Grt, Bt, Ky	Rt, Ap, Mnz, Zrn	Mnz: 1539±8	Metamorphism	U-Pb SIMS	5e
							Mnz: 1052±4, 1025±9	Metamorphism	U-Pb SIMS	5d
B99143	Hensmoen	Gneiss	567300	6678100	Qtz, Kfs, Amp, Pl, Grt, Bt, Aln	Ttn, opaque, Ap, Zrn	Zrn core: 1495±11	Magmatism	U-Pb SIMS	5f
							Zrn rim: 1091±18	Metamorphism	U-Pb SIMS	5g
							Ttn: 1043±8	Metamorphism	U-Pb ID-TIMS	5h
B99140	Hensmoen	Gneiss	568100	6678000	Qtz, Kfs, Pl, Bt, Amp, Grt	Ttn, Aln, opaque, Ap, Zrn	Ttn: 1040 ±14, 1024 ±9	Metamorphism	U-Pb ID-TIMS	5h
Vardefjell Shear Zone										
B99111	Flå	Banded gneiss	526001	6699230	Qtz, Pl, Amp, Bt	Ttn, Ap, Zrn	Zrn core: 1528±16	Magmatism	U-Pb SIMS	7a
							Zrn rim: 1012±7	Metamorphism	U-Pb SIMS	7b
B99114	Flå	Banded gneiss	524800	6703500	Qtz, Kfs, Pl, Amp, Bt, Grt	Aln, Ttn, Ap, Zrn	Zrn: 1507±14	Magmatism	U-Pb SIMS	7c
							Zrn: 1008±14	Metamorphism	U-Pb SIMS	7d
							Ttn: 985±5	Metamorphism	U-Pb ID-TIMS	7e
Telemarkia Terrane, Telemark Sector										
B99130	Noresund	Amphibolite	534700	6676600	Pl, Amp, Bt, Grt, opaque	Ap, Zrn	Zrn: 1014±1	Metamorphism	U-Pb ID-TIMS	7f
Telemarkia Terrane, Rogaland-Vest Agder Sector										
B0234	Rygnestad	Metapelite	413912	6571615	Pl, Qtz, Grt, Bt, Sil, Crd (pinite)	Ap, Zrn, Mnz, opaque	Mnz: 1005 ±7	Metamorphism	U-Pb LA-ICPMS	8a
B0128	Knaben II	Granitic gneiss	388374	6503807	Qtz, Kfs, Bt, Pl, Moly, opaque	Ap, Zrn, Cal, Ep-Aln, Mnz	Mnz: 1002±7	Metamorphism	U-Pb SIMS	8c
B00158	Øvstabø	Granulite	354545	6524603	Qtz, Kfs, Pl, Opx, Grt, Bt	Opaque, Ap, Zrn, Mnz	Mnz: 1032±5; 990±8	Metamorphism	U-Pb SIMS	8b
B185	Sirdal	Augen gneiss	365350	6492950	Qtz, Pl, Kfs, Bt, Amp, Cpx	Opaque, Ap, Zrn, Ttn, Aln, Mnz	Mnz: 927±5, 924±5	Metamorphism	Th-Pb ID-TIMS	9
B135	Feda	Augen gneiss	371700	6462500	Qtz, Pl, Kfs, Bt	Opaque, Ap, Zrn, Ttn, Mnz	Mnz: 999±5, 922±5	Metamorphism	Th-Pb ID-TIMS	9
B113	Feda	Augen gneiss	370650	6462000	Qtz, Pl, Kfs, Bt, Amp, Cpx	Opaque, Ap, Zrn, Ttn, Mnz	Mnz: 914±4, 910±9	Metamorphism	Th-Pb ID-TIMS	9
B191	Drangsdalen	Augen gneiss	351500	6482800	Qtz, Pl, Kfs, Bt, Opx	Opaque, Ap, Zrn, Ttn, Mnz	Mnz: 997±5, 947±5	Metamorphism	Th-Pb ID-TIMS	9
B649	Gyadalen	Granulite	343700	6497000	Qtz, Pl, Kfs, Opx, Cpx	Opaque, Ap, Zrn, Mnz	Mnz: 1013±5, 980±5	Metamorphism	Th-Pb ID-TIMS	9

(1) UTM WGS84 coordinate, zone 32
(2) Mineral listed in decreasing abundance. Aln: allanite; Amp: amphibole; Ap: apatite; Bt: biotite; Cal: calcite; Cpx: clinopyroxene; Crd: cordierite; Ep: epidote; Grt: garnet; Kfs: K-feldspar; Ky: kyanite; Mnz: monazite; Moly: molybdenite; Ms: muscovite; Opx: orthopyroxene; Pl: plagioclase; Qtz: quartz; Sil: sillimanite; Trm: tourmaline; Ttn: titanite; Xnt: xenotime; Zrn: zircon.
(3) For Th-Pb ID-TIMS, the listed age is 208Pb/232Th age, equivalent to both 207Pb/235U and 206Pb/238U ages
(4) Figure reporting concordia diagram

Table 1. Sample location and summary of geochronological data.

Table 2. SIMS U-Pb data on zircon

Spot ID	zone (1)	[U] (ppm)	[Th] (ppm)	[Pb] (ppm)	*f*206 (%) (2)	208Pb/ 206Pb	±1σ (3)	207Pb/ 235U	±1σ	206Pb/ 238U	±1σ	R (4)	207Pb/ 206Pb	±1σ	206/238 Age (Ma) (5)	±1σ	207/235 Age (Ma) (5)	±1σ	207/206 Age (Ma) (5)	±1σ	Disc. (%) (6)
B99143. Grt-Amp gneiss. Idefjorden Terrane																					
B1.1	c	67	33	17	0.11	0.1526	0.0038	3.2111	0.1046	0.23914	0.00620	0.86	0.0974	0.0016	1382	32	1460	26	1575	32	12
B13.2	c	78	44	22	0.04	0.1850	0.0069	3.3422	0.1014	0.25626	0.00673	0.92	0.0946	0.0012	1471	35	1491	24	1520	23	3
B4.1	c	146	90	42	0.16	0.1882	0.0015	3.3849	0.0936	0.26123	0.00675	0.97	0.0940	0.0007	1496	35	1501	22	1508	13	1
A1.1	c	163	124	49	0.02	0.2365	0.0025	3.4093	0.0918	0.26375	0.00670	0.97	0.0938	0.0006	1509	34	1507	21	1503	12	0
A9.2	c	305	69	82	0.04	0.0697	0.0006	3.4392	0.0909	0.26783	0.00672	0.98	0.0931	0.0005	1530	34	1513	21	1491	11	-3
B19.1	c	303	110	80	0.19	0.1080	0.0019	3.2826	0.0930	0.25715	0.00683	0.97	0.0926	0.0007	1475	35	1477	22	1479	14	0
A6.1	c	41	41	13	0.29	0.3221	0.0074	3.2115	0.1215	0.25302	0.00718	0.82	0.0921	0.0020	1454	37	1460	30	1469	42	1
A8.1	r	552	4	95	0.02	0.0036	0.0009	1.9565	0.0594	0.18457	0.00465	0.89	0.0769	0.0011	1092	25	1101	21	1118	28	2
B13.1	r	446	4	77	0.09	0.0038	0.0010	1.9365	0.0528	0.18606	0.00472	0.96	0.0755	0.0006	1100	26	1094	18	1081	15	-2
A6.2	r	459	11	82	0.03	0.0097	0.0005	1.9919	0.0549	0.19160	0.00487	0.96	0.0754	0.0006	1130	26	1113	19	1079	16	-5
B99111. Grt-Amp banded gneiss. Vardefjell Shear Zone																					
F7.1	ic	67	15	18	0.02	0.0718	0.0015	3.7614	0.1042	0.27247	0.00692	0.95	0.1001	0.0008	1553	35	1585	22	1626	16	4
F6.1	ic	68	15	20	0.13	0.0737	0.0021	3.9292	0.1275	0.28712	0.00732	0.85	0.0993	0.0017	1627	37	1620	27	1610	32	-1
B2.1	ic	147	57	43	0.09	0.1178	0.0010	3.7254	0.0980	0.27736	0.00703	0.98	0.0974	0.0005	1578	36	1577	21	1575	9	0
B8.1	c	65	15	17	0.25	0.0705	0.0024	3.5230	0.1109	0.26476	0.00680	0.88	0.0965	0.0015	1514	35	1532	25	1558	29	3
C7.1	c	116	25	29	0.39	0.0644	0.0018	3.3595	0.0915	0.25378	0.00643	0.96	0.0960	0.0007	1458	33	1495	22	1548	14	6
F5.1	c	70	19	19	0.44	0.0865	0.0045	3.5220	0.1227	0.26676	0.00695	0.82	0.0958	0.0019	1524	35	1532	28	1543	38	1
F2.1	c	38	11	11	0.28	0.0944	0.0028	3.6385	0.1212	0.27800	0.00769	0.89	0.0949	0.0015	1581	39	1558	27	1527	29	-4
C8.1	c	92	24	26	0.30	0.0766	0.0020	3.6191	0.1058	0.27680	0.00730	0.94	0.0948	0.0009	1575	37	1554	24	1525	18	-3
D1.1	c	242	116	71	0.10	0.1496	0.0012	3.5689	0.0940	0.27426	0.00689	0.98	0.0944	0.0005	1562	35	1543	21	1516	10	-3
D8.3	c	52	11	13	0.38	0.0690	0.0053	3.3080	0.1325	0.25561	0.00754	0.81	0.0939	0.0022	1467	39	1483	32	1505	45	3
D8.1	mix	56	13	14	0.65	0.0694	0.0033	3.0158	0.0985	0.24373	0.00640	0.87	0.0897	0.0015	1406	33	1412	25	1420	32	1
F7.2	mix	366	2	61	0.01	0.0030	0.0009	1.8848	0.0528	0.17989	0.00455	0.94	0.0760	0.0007	1066	25	1076	19	1095	19	3
E1.2	p	265	2	41	0.11	0.0031	0.0012	1.6901	0.0475	0.16584	0.00426	0.95	0.0739	0.0006	989	24	1005	18	1039	17	5
D7.2	r	392	1	62	0.01	0.0016	0.0005	1.7428	0.0455	0.17143	0.00431	0.98	0.0737	0.0003	1020	24	1024	17	1034	9	1
D8.2	r	456	4	73	0.04	0.0030	0.0006	1.7446	0.0456	0.17189	0.00430	0.98	0.0736	0.0004	1022	24	1025	17	1031	10	1
F1.1	p	686	9	107	0.08	0.0031	0.0002	1.7116	0.0447	0.16886	0.00425	0.99	0.0735	0.0003	1006	23	1013	17	1028	9	2
D1.2	r	680	5	110	0.07	0.0016	0.0007	1.7737	0.0475	0.17515	0.00445	0.98	0.0735	0.0004	1040	24	1036	18	1026	12	-1
B8.2	r	470	1	77	0.04	0.0003	0.0007	1.7825	0.0493	0.17666	0.00450	0.96	0.0732	0.0006	1049	25	1039	18	1019	16	-3
C9.1	p	458	4	71	0.05	0.0033	0.0006	1.6969	0.0455	0.16819	0.00424	0.97	0.0732	0.0005	1002	23	1007	17	1019	13	2
E5.1	p	383	5	60	0.04	0.0056	0.0008	1.6896	0.0472	0.16765	0.00429	0.95	0.0731	0.0006	999	24	1005	18	1017	17	2
D6.2	r	742	2	113	0.07	-0.0001	0.0003	1.6627	0.0432	0.16597	0.00418	0.99	0.0727	0.0003	990	23	994	17	1004	8	1
F5.2	r	353	1	57	0.01	0.0023	0.0006	1.7401	0.0498	0.17418	0.00439	0.93	0.0725	0.0008	1035	24	1024	19	999	22	-4
F6.2	r	358	1	60	0.18	-0.0003	0.0013	1.8013	0.0515	0.18038	0.00457	0.93	0.0724	0.0008	1069	25	1046	19	998	21	-7
C8.2	r	356	1	57	0.09	0.0002	0.0004	1.7312	0.0460	0.17337	0.00435	0.97	0.0724	0.0004	1031	24	1020	17	998	12	-3
E1.1	p	267	2	41	0.10	0.0023	0.0006	1.6473	0.0430	0.16555	0.00416	0.99	0.0722	0.0003	988	23	989	17	991	9	0
B2.2	r	435	3	68	0.11	0.0010	0.0006	1.6914	0.0448	0.17000	0.00427	0.98	0.0722	0.0004	1012	24	1005	17	991	12	-2
A4.1	p	439	8	61	0.07	0.0049	0.0011	1.5004	0.0508	0.15088	0.00428	0.89	0.0721	0.0011	906	24	931	21	989	32	8
D2.1	p	536	4	84	0.11	0.0015	0.0004	1.6890	0.0446	0.17007	0.00429	0.98	0.0720	0.0004	1013	24	1004	17	987	11	-3

B99114. Grt-Amp banded gneiss. Vardefjell Shear Zone																					
A1.1	c	80	52	23	0.02	0.2041	0.0031	3.4776	0.1088	0.25992	0.00727	0.94	0.0970	0.0011	1489	37	1522	25	1568	21	5
B12.1	c	195	160	57	0.34	0.2536	0.0032	3.3282	0.1058	0.25238	0.00693	0.92	0.0956	0.0012	1451	36	1488	25	1541	25	6
B14.1	c	198	167	62	0.13	0.2734	0.0035	3.4666	0.1025	0.26482	0.00717	0.95	0.0949	0.0009	1515	37	1520	24	1527	17	1
A14.1	c	70	50	22	0.56	0.2029	0.0037	3.7147	0.1263	0.28435	0.00821	0.90	0.0948	0.0014	1613	41	1575	28	1523	28	-6
A10.1	c	81	51	23	0.35	0.1957	0.0029	3.3203	0.1151	0.25580	0.00713	0.87	0.0941	0.0016	1468	37	1486	27	1511	33	3
B8.1	c	124	80	36	0.21	0.1990	0.0023	3.3513	0.0981	0.25837	0.00689	0.95	0.0941	0.0009	1482	35	1493	23	1510	17	2
B5.1	c	206	139	61	0.13	0.2075	0.0018	3.4059	0.0884	0.26281	0.00659	0.99	0.0940	0.0004	1504	34	1506	21	1508	8	0
B11.1	c	239	187	71	0.05	0.2485	0.0024	3.3020	0.0910	0.25799	0.00664	0.97	0.0928	0.0007	1480	34	1482	22	1484	14	0
A2.2	r	300	4	47	0.10	0.0066	0.0008	1.6917	0.0469	0.16773	0.00429	0.96	0.0732	0.0006	1000	24	1005	18	1018	16	2
B4.2	r	119	5	18	0.44	0.0080	0.0029	1.6636	0.0640	0.16651	0.00442	0.77	0.0725	0.0018	993	24	995	25	999	51	1
B2.2	r	158	3	24	0.17	0.0066	0.0009	1.6496	0.0475	0.16517	0.00420	0.93	0.0724	0.0008	985	23	989	18	998	22	1
A4.2	r	123	4	20	0.66	0.0043	0.0037	1.7515	0.0653	0.17546	0.00468	0.79	0.0724	0.0017	1042	26	1028	24	997	47	-4
A10.2	r	187	5	30	0.26	0.0091	0.0023	1.7059	0.0553	0.17156	0.00443	0.86	0.0721	0.0012	1021	24	1011	21	989	34	-3
A14.2	r	136	2	22	0.41	0.0030	0.0019	1.7177	0.0611	0.17381	0.00471	0.83	0.0717	0.0014	1033	26	1015	23	977	41	-6
B14.2	r	189	4	30	0.40	0.0036	0.0018	1.6942	0.0546	0.17458	0.00455	0.87	0.0704	0.0011	1037	25	1006	21	940	33	-10

(1) Zone: c: core. r: rim. p: poorly zoned zircon. ic: inherited core. mix: analysis straddles core-rim interface or fracture
(2) *f* 206Pb (%) indicates the percentage of common 206Pb in the total measured 206Pb.
(3) Uncertainties are reported at the 1sigma level and are calculated by numerical propagation of all known sources of error (Stern. 1997)
(4) Correlation coefficient of errors in isotopic ratios
(5) Ages calculated using the 204-method for common Pb correction unless otherwise noted.
(6) Discordance = 100-(100 x (206Pb/238U age)/(207Pb/206Pb age).

Table 2. SIMS U-Pb data on zircon.

at the Geological Survey of Canada following Davis et al. (1998) (Table 4). Typical procedural blank for Pb was 2 pg. In addition, ID-TIMS U-Pb analyses were made on air-abraded zircon fractions, and non-abraded titanite fractions (Table 4). U-Pb analytical procedures were modified after Parrish et al. (1987) and Davis et al. (1997). Modifications included the use of Savillex dissolution vials for titanite analyses and the use of microcolumns for cation exchange chemistry for zircon analyses. Typical procedural blank for Pb was 2-5 pg for zircon analyses and 5-10 pg for titanite analyses. ID-TIMS data were corrected for procedural and lattice common Pb using the ^{204}Pb concentration. For lattice common Pb, isotopic composition at the time of crystallization is estimated following the evolution curve of Stacey and Kramers (1975).

LA-ICPMS analyses of monazite were performed at the Geological Survey of Norway (Table 5) following Bingen et al. (2005). The data were collected on a Finnigan Element I single collector sector ICPMS, fed by a Finnigan 266 nm laser microsampler. Analyses were done with a laser beam rastered over an area of c. 40 x 60 μm over the crystal section. Isotopes ^{202}Hg, ^{204}(Hg + Pb), ^{206}Pb, ^{207}Pb, ^{208}Pb, ^{238}U and ^{232}Th were measured in a time-resolved counting scanning mode for 60 sec. The interference between ^{204}Pb and ^{204}Hg contained in the Ar gas was corrected by monitoring ^{202}Hg. A 60 sec gas blank analysis was performed between each analysis. The measured isotope ratios were corrected for element- and mass-bias effects using the Geostandard 91500 reference zircon. Common Pb detected in the analyses is mainly attributed to contamination at the surface of the sample and to instrumental contamination including carrier (He) and plasma gases (Ar). A common Pb correction was thus applied using the ^{204}Pb analysis, and the measured blank isotopic composition. Ablation related variation in element fractionation of up to several percent is unavoidable with the instrumentation used. Therefore, the ^{207}Pb/^{206}Pb age is regarded as the most reliable age estimate for LA-ICPMS data.

Ages were derived with the following decay constants: λ^{238}U =1.55125 10^{-10} y^{-1}; λ^{235}U =9.8485 10^{-10} y^{-1}; λ^{232}Th =4.9475 10^{-11} y^{-1}, ^{238}U/^{235}U =137.88. The ISOPLOT program (Ludwig 2001) was used to generate concordia diagrams and derive ages. For ion microprobe data, concordia ages (Ludwig 1998) were calculated for all samples. They are quoted with the combined MSWD of concordance and equivalence. All errors on ages are quoted at the 2σ or 95% confidence levels, as selected by ISOPLOT. Except for the purpose of comparison with Re-Os data, the errors on U-Pb data do not include propagation of uncertainty on the decay constants. The consistency of results on monazite obtained by the three different analytical methods (SIMS, LA-ICPMS and ID-TIMS) has been evaluated with two of the samples (Table 6).

Table 3. SIMS U-Pb data on monazite

Spot Id	zone (1)	206Pb/ 204Pb	*f*206 (%) (2)	208Pb/ 206Pb	±1σ (3)	207Pb/ 235U	±1σ	206Pb/ 238U	±1σ	R (4)	207Pb/ 206Pb	±1σ	206/238 Age (Ma) (5)	±1σ	207/23 5 Age (Ma)	±1σ	207/206 Age (Ma)	±1σ	Disc. (%) (6)
B0109. Grt-Sil metapelitic gneiss. Bamble Terrane																			
14,1	1	30750	0.00055	2.187	0.009	2.119	0.029	0.1965	0.0024	0.95	0.07821	0.00034	1156	13	1155	9	1152	9	0
8,1	1	14821	0.00113	3.989	0.020	2.071	0.030	0.1925	0.0025	0.93	0.07805	0.00042	1135	14	1139	10	1148	11	1
9,1	1	22665	0.00074	3.806	0.018	2.020	0.029	0.1879	0.0024	0.94	0.07797	0.00039	1110	13	1122	10	1146	10	3
29,1	1	9958	0.00169	5.943	0.030	2.034	0.033	0.1902	0.0027	0.93	0.07756	0.00047	1123	15	1127	11	1136	12	1
20,1	1	18228	0.00092	3.268	0.021	2.075	0.029	0.1941	0.0024	0.94	0.07753	0.00036	1143	13	1140	9	1135	9	-1
5,1	1	15430	0.00109	4.102	0.017	2.049	0.030	0.1917	0.0025	0.93	0.07750	0.00040	1131	13	1132	10	1134	10	0
16,1	1	41771	0.00040	1.661	0.007	2.099	0.028	0.1965	0.0025	0.96	0.07748	0.00030	1157	13	1149	9	1134	8	-2
14,2	1	17358	0.00097	3.960	0.018	2.040	0.031	0.1914	0.0026	0.94	0.07729	0.00040	1129	14	1129	10	1129	10	0
3,1	1	29412	0.00057	1.827	0.010	2.048	0.028	0.1925	0.0023	0.94	0.07715	0.00036	1135	13	1132	9	1125	9	-1
20,2	1	17851	0.00094	4.067	0.019	2.046	0.031	0.1926	0.0026	0.94	0.07703	0.00039	1135	14	1131	10	1122	10	-1
3,2	1	8278	0.00204	7.622	0.037	1.983	0.033	0.1876	0.0026	0.90	0.07667	0.00055	1108	14	1110	11	1113	14	0
2,1	1	15492	0.00109	5.033	0.022	2.023	0.030	0.1920	0.0025	0.92	0.07642	0.00046	1132	14	1123	10	1106	12	-2
2,2		14861	0.00114	3.649	0.019	2.064	0.031	0.1970	0.0026	0.92	0.07600	0.00043	1159	14	1137	10	1095	11	-6
B01011. Grt-Sil metapelitic gneiss. Bamble Terrane																			
20,1	1	26392	0.00064	1.656	0.006	2.036	0.022	0.1897	0.0020	0.99	0.07782	0.00015	1120	11	1128	8	1142	4	2
3,1	1	24301	0.00069	1.433	0.006	2.026	0.022	0.1890	0.0019	0.98	0.07772	0.00018	1116	11	1124	7	1140	5	2
16,1	1	26330	0.00064	1.800	0.006	2.045	0.021	0.1908	0.0019	0.99	0.07772	0.00013	1126	11	1131	7	1140	3	1
24,1	1	26048	0.00065	1.766	0.005	2.047	0.022	0.1911	0.0020	0.98	0.07767	0.00014	1128	11	1131	7	1138	4	1
16,2	1	12984	0.00130	5.433	0.022	2.055	0.024	0.1930	0.0020	0.95	0.07721	0.00029	1138	11	1134	8	1127	7	-1
1,1	1	15129	0.00111	4.605	0.017	2.033	0.024	0.1916	0.0021	0.96	0.07697	0.00027	1130	11	1127	8	1120	7	-1
20,2	1	9866	0.00171	5.235	0.020	1.987	0.024	0.1877	0.0021	0.95	0.07678	0.00029	1109	11	1111	8	1116	7	1
24,2		8238	0.00205	5.778	0.024	2.028	0.024	0.1929	0.0021	0.93	0.07625	0.00034	1137	11	1125	8	1102	9	-3
B0116. Bt-Ms quartzite. Bamble Terrane																			
3,2	1	10226	0.00164	4.975	0.027	2.048	0.037	0.1896	0.0030	0.93	0.07834	0.00050	1119	16	1132	12	1156	13	3
12,1	1	21825	0.00077	2.070	0.012	2.084	0.032	0.1935	0.0027	0.95	0.07809	0.00039	1140	14	1143	11	1149	10	1
7,1	1	13065	0.00129	3.669	0.027	2.021	0.041	0.1894	0.0033	0.92	0.07742	0.00064	1118	18	1123	14	1132	16	1
19,1	1	16767	0.00100	3.366	0.020	2.018	0.027	0.1902	0.0023	0.92	0.07695	0.00041	1122	12	1122	9	1120	11	0
12,2	2	7325	0.00230	8.311	0.044	1.962	0.033	0.1865	0.0026	0.90	0.07630	0.00057	1102	14	1103	11	1103	15	0
10,1	2	15501	0.00109	2.694	0.012	1.982	0.024	0.1884	0.0021	0.95	0.07630	0.00028	1113	11	1109	8	1103	7	-1
18,1	2	21231	0.00079	2.135	0.009	1.962	0.023	0.1866	0.0020	0.95	0.07624	0.00028	1103	11	1102	8	1101	7	0
19,2	2	13812	0.00122	3.632	0.021	1.971	0.026	0.1878	0.0022	0.93	0.07611	0.00038	1110	12	1106	9	1098	10	-1
19,3	2	10993	0.00154	3.816	0.018	2.027	0.027	0.1936	0.0023	0.93	0.07596	0.00038	1141	12	1125	9	1094	10	-4
7,2	2	4124	0.00410	15.007	0.101	1.994	0.044	0.1915	0.0033	0.86	0.07550	0.00084	1130	18	1113	15	1082	23	-4
3,1		11598	0.00146	3.969	0.019	2.021	0.032	0.1951	0.0028	0.94	0.07514	0.00041	1149	15	1123	11	1072	11	-7
12,3		1818	0.00938	30.366	0.191	1.862	0.055	0.1862	0.0028	0.62	0.07251	0.00169	1101	15	1068	20	1000	48	-10

B0024. Sil quartzite. Bamble Terrane. analyses uncorrected for common Pb																			
4,3	1	34447		16.424	0.187	2.077	0.041	0.1932	0.0029	0.83	0.07796	0.00085	1139	16	1141	13	1146	22	1
16,1	1	2586		38.476	0.189	2.015	0.037	0.1880	0.0030	0.91	0.07773	0.00059	1111	16	1121	13	1140	15	3
18,1	1	14894		26.436	0.143	2.117	0.032	0.1977	0.0027	0.94	0.07767	0.00041	1163	14	1154	10	1139	11	-2
4,2	1	9295		9.723	0.027	2.019	0.026	0.1886	0.0022	0.97	0.07766	0.00026	1114	12	1122	9	1138	7	2
18,2	1	17170		25.689	0.336	2.068	0.030	0.1938	0.0025	0.93	0.07738	0.00043	1142	13	1138	10	1131	11	-1
6,2	1	4137		21.112	0.087	2.015	0.034	0.1889	0.0028	0.94	0.07736	0.00045	1115	15	1121	11	1130	12	1
22,2	1	19924		19.475	0.173	2.045	0.026	0.1919	0.0022	0.94	0.07731	0.00035	1131	12	1131	9	1129	9	0
8,1	1	44823		5.535	0.057	2.109	0.025	0.1980	0.0021	0.95	0.07726	0.00028	1164	11	1152	8	1128	7	-3
6,1	1	4560		13.916	0.050	1.985	0.029	0.1872	0.0024	0.94	0.07691	0.00039	1106	13	1110	10	1119	10	1
11,2	1	3459		19.538	0.091	1.961	0.033	0.1851	0.0027	0.90	0.07686	0.00056	1095	15	1102	11	1117	15	2
11,1	1	4124		19.178	0.118	1.997	0.035	0.1885	0.0029	0.93	0.07684	0.00048	1113	16	1115	12	1117	12	0
4,1	1	4535		18.048	0.083	2.029	0.033	0.1919	0.0027	0.93	0.07670	0.00047	1132	15	1125	11	1113	12	-2
6,4		14680		14.872	0.138	2.145	0.028	0.2029	0.0023	0.92	0.07667	0.00039	1191	13	1163	9	1113	10	-7
6,3	1	12925		19.457	0.335	1.998	0.032	0.1897	0.0025	0.87	0.07638	0.00062	1120	13	1115	11	1105	16	-1
11,3	1	19940		18.282	0.153	2.016	0.032	0.1915	0.0025	0.88	0.07633	0.00060	1130	14	1121	11	1104	16	-2
16,2	1	11490		37.636	0.243	2.034	0.031	0.1935	0.0025	0.91	0.07622	0.00049	1140	14	1127	10	1101	13	-4
22,1		16697		17.697	0.119	2.103	0.028	0.2007	0.0024	0.92	0.07599	0.00042	1179	13	1150	9	1095	11	-8
B0030. Sil nodular gneiss. Kongsberg Terrane																			
15,1	1	88496	0.00019	0.431	0.005	1.967	0.027	0.1862	0.0023	0.95	0.07662	0.00034	1101	13	1104	9	1111	9	1
7,2	1	26164	0.00064	3.220	0.024	1.945	0.033	0.1846	0.0026	0.90	0.07643	0.00056	1092	14	1097	11	1106	15	1
6,1	1	18409	0.00092	3.415	0.017	1.921	0.029	0.1832	0.0024	0.92	0.07607	0.00045	1084	13	1089	10	1097	12	1
16,1	1	22589	0.00075	2.312	0.014	1.880	0.028	0.1796	0.0024	0.93	0.07594	0.00043	1065	13	1074	10	1093	11	3
18,1	1	17464	0.00097	3.873	0.016	1.985	0.028	0.1896	0.0024	0.94	0.07594	0.00036	1119	13	1110	10	1093	9	-2
15,2	1	40048	0.00042	1.278	0.008	1.931	0.027	0.1845	0.0023	0.94	0.07590	0.00036	1091	12	1092	9	1092	9	0
3,2	1	37175	0.00045	1.385	0.007	1.940	0.025	0.1857	0.0022	0.94	0.07576	0.00032	1098	12	1095	9	1089	9	-1
7,1	1	26406	0.00064	2.683	0.013	1.929	0.027	0.1851	0.0023	0.94	0.07557	0.00036	1095	13	1091	9	1084	10	-1
26,2	1	20387	0.00083	2.646	0.015	1.909	0.029	0.1834	0.0025	0.94	0.07551	0.00040	1085	13	1084	10	1082	11	0
18,2		10380	0.00163	6.201	0.026	1.967	0.030	0.1914	0.0026	0.94	0.07452	0.00040	1129	14	1104	10	1055	11	-7
26,1		5955	0.00285	10.827	0.045	1.910	0.031	0.1867	0.0026	0.92	0.07420	0.00047	1104	14	1085	11	1047	13	-5
3,1		4513	0.00377	15.335	0.072	1.913	0.034	0.1892	0.0028	0.88	0.07335	0.00062	1117	15	1086	12	1024	17	-9
B99137. Grt-Ky metapelitic gneiss. Idefjorden Terrane																			
25,1	1	39526	0.00041	1.413	0.006	3.524	0.046	0.2674	0.0034	0.99	0.09557	0.00020	1528	17	1533	10	1539	4	1
3,1	mix	22416	0.00074	3.452	0.015	2.410	0.034	0.2088	0.0027	0.95	0.08370	0.00037	1222	14	1246	10	1286	9	5
30,1	mix	29019	0.00057	2.066	0.007	2.335	0.028	0.2044	0.0023	0.98	0.08282	0.00020	1199	12	1223	8	1265	5	5
17,1	2	61538	0.00028	0.743	0.003	1.819	0.021	0.1765	0.0019	0.98	0.07476	0.00017	1048	10	1053	7	1062	5	1
18,1	2	60976	0.00028	0.736	0.003	1.800	0.020	0.1747	0.0019	0.99	0.07474	0.00013	1038	10	1045	7	1061	3	2
25,2	2	53619	0.00032	1.089	0.004	1.799	0.021	0.1750	0.0019	0.97	0.07455	0.00022	1040	10	1045	8	1057	6	2
22,1	2	56211	0.00030	0.898	0.004	1.780	0.020	0.1734	0.0019	0.98	0.07446	0.00019	1031	10	1038	7	1054	5	2
4,1	2	44425	0.00038	1.172	0.004	1.785	0.020	0.1741	0.0019	0.98	0.07438	0.00016	1035	10	1040	7	1052	4	2
8,1	2	35486	0.00048	1.437	0.006	1.806	0.022	0.1763	0.0020	0.97	0.07430	0.00021	1047	11	1048	8	1050	6	0
5,1	2	28209	0.00060	1.930	0.008	1.778	0.021	0.1736	0.0020	0.97	0.07429	0.00021	1032	11	1037	8	1049	6	2
30,2	2	41494	0.00041	1.309	0.005	1.771	0.020	0.1729	0.0019	0.98	0.07429	0.00016	1028	10	1035	7	1049	4	2
20,2	2	33047	0.00051	1.817	0.006	1.815	0.023	0.1774	0.0022	0.98	0.07420	0.00021	1053	12	1051	9	1047	6	-1

20,1	2	21336	0.00080	1.688	0.005	1.826	0.021	0.1788	0.0019	0.98	0.07408	0.00017	1060	11	1055	8	1044	5	-2
3,2	3	29499	0.00058	1.618	0.007	1.739	0.021	0.1715	0.0019	0.97	0.07351	0.00022	1021	11	1023	8	1028	6	1
13,1	3	22326	0.00076	2.156	0.010	1.769	0.023	0.1753	0.0021	0.95	0.07317	0.00029	1041	11	1034	8	1019	8	-2
B00158. Grt granulite. Telemarkia Terrane. Rogaland-Vest Agder Sector																			
7,1		52938	0.00032	3.500	0.041	1.496	0.028	0.1464	0.0022	0.85	0.07413	0.00075	881	12	929	12	1045	20	16
1,1	1	17394	0.00098	4.253	0.017	1.775	0.021	0.1738	0.0018	0.95	0.07410	0.00027	1033	10	1036	8	1044	8	1
8,2	1	20076	0.00085	3.257	0.014	1.753	0.021	0.1716	0.0019	0.95	0.07409	0.00028	1021	10	1028	8	1044	8	2
4,1	1	21459	0.00079	2.674	0.011	1.757	0.020	0.1727	0.0019	0.96	0.07380	0.00024	1027	10	1030	8	1036	7	1
23,1	1	16194	0.00105	3.868	0.016	1.761	0.021	0.1733	0.0019	0.94	0.07369	0.00031	1030	10	1031	8	1033	8	0
3,1	1	13877	0.00123	3.735	0.014	1.770	0.021	0.1749	0.0019	0.96	0.07340	0.00024	1039	10	1035	8	1025	7	-1
2,1	1	14286	0.00119	4.464	0.018	1.742	0.022	0.1726	0.0019	0.93	0.07323	0.00033	1026	10	1024	8	1020	9	-1
3,2	2	14669	0.00116	3.680	0.012	1.673	0.019	0.1675	0.0018	0.96	0.07245	0.00022	998	10	998	7	999	6	0
7,2	2	15610	0.00109	6.918	0.035	1.590	0.020	0.1592	0.0018	0.92	0.07242	0.00036	952	10	966	8	998	10	5
23,3	2	18096	0.00094	3.212	0.012	1.657	0.020	0.1661	0.0019	0.95	0.07231	0.00029	991	10	992	8	995	8	0
4,2	2	12829	0.00133	4.624	0.015	1.654	0.019	0.1663	0.0018	0.95	0.07214	0.00025	992	10	991	7	990	7	0
8,1	2	15726	0.00109	3.061	0.016	1.614	0.018	0.1623	0.0017	0.97	0.07210	0.00020	970	10	976	7	989	6	2
23,2	2	16918	0.00101	3.125	0.011	1.640	0.020	0.1652	0.0018	0.94	0.07200	0.00030	986	10	986	8	986	9	0
1,2	2	5445	0.00314	11.119	0.038	1.685	0.024	0.1699	0.0019	0.87	0.07192	0.00051	1011	11	1003	9	984	14	-3
2,2		7357	0.00232	8.748	0.026	1.712	0.023	0.1731	0.0021	0.94	0.07174	0.00033	1029	11	1013	9	979	9	-5
B01028. Molybdenite granitic gneiss. Telemarkia Terrane. Rogaland-Vest Agder Sector																			
10,2	1	16242	0.00105	3.481	0.016	1.661	0.021	0.1639	0.0018	0.94	0.07350	0.00032	979	10	994	8	1028	9	5
21,1	1	8689	0.00196	7.677	0.034	1.667	0.023	0.1648	0.0019	0.92	0.07334	0.00040	984	11	996	9	1023	11	4
26,2	1	23901	0.00071	3.176	0.014	1.702	0.021	0.1683	0.0019	0.95	0.07334	0.00029	1003	10	1009	8	1023	8	2
16,1	1	15232	0.00112	4.497	0.013	1.678	0.019	0.1660	0.0018	0.96	0.07330	0.00022	990	10	1000	7	1022	6	3
28,1	1	18195	0.00094	3.694	0.013	1.694	0.020	0.1682	0.0018	0.96	0.07301	0.00025	1002	10	1006	7	1014	7	1
20,1	1	19900	0.00086	2.870	0.012	1.669	0.020	0.1659	0.0018	0.95	0.07296	0.00028	990	10	997	8	1013	8	2
11,1	1	19478	0.00088	3.937	0.014	1.686	0.019	0.1681	0.0018	0.96	0.07276	0.00023	1001	10	1003	7	1007	7	1
29,2	1	11858	0.00144	5.059	0.016	1.684	0.020	0.1683	0.0018	0.94	0.07259	0.00029	1003	10	1003	8	1003	8	0
15,1	1	10444	0.00163	4.698	0.022	1.677	0.022	0.1677	0.0019	0.93	0.07253	0.00036	999	11	1000	8	1001	10	0
10,1	1	16609	0.00103	3.610	0.014	1.682	0.021	0.1683	0.0019	0.93	0.07246	0.00033	1003	10	1002	8	999	9	0
21,2	1	12742	0.00134	4.986	0.022	1.643	0.022	0.1648	0.0019	0.93	0.07230	0.00037	983	11	987	8	995	10	1
1,1		80064	0.00021	5.192	0.061	1.200	0.023	0.1243	0.0018	0.84	0.07003	0.00073	755	11	801	11	929	22	19
29,1	2	13167	0.00131	5.421	0.024	1.434	0.018	0.1502	0.0017	0.93	0.06925	0.00033	902	9	903	8	906	10	0

(1) Zone: Age domains numeroted from 1 to 3. mix: analysis stradles core-rim interface or fracture
(2) *f*206Pb (%) indicates the percentage of common 206Pb in the total measured 206Pb.
(3) Uncertainties are reported at the 1sigma level and are calculated by numerical propagation of all known sources of error (Stern. 1997)
(4) Correlation coefficient of errors in isotopic ratios
(5) Ages calculated using the 204-method for common Pb correction unless otherwise noted.
(6) Discordance = 100-(100 x (206Pb/238U age)/(207Pb/206Pb age).

Table 3. SIMS U-Pb data on monazite.

Table 4. ID-TIMS Th-U-Pb data on monazite. zircon and titanite

																	Apparent Age (Ma)								
Fraction	Wt.	U	Th	Pbr	$^{206}Pb/$	Pbc	$^{208}Pb/$	$^{207}Pb/$	±1σ	$^{206}Pb/$	±1σ	R	$^{207}Pb/$	±1σ	$^{208}Pb/$	±1σ	$^{206}Pb/$	±2σ	$^{207}Pb/$	±2σ	$^{207}Pb/$	±2σ	Disc	$^{208}Pb/$	±2σ
Id	(µg)	(ppm)	(ppm)	(ppm)	^{204}Pb	(pg)	^{206}Pb	^{235}U		^{238}U			^{206}Pb		^{232}Th		^{238}U		^{235}U		^{206}Pb		(%)	^{232}Th	
		(1)	(1)	(2)		(2)	(3)					(4)											(5)		
B0109, Z7358, Grt-Sil metapelitic gneiss, Bamble Terrane; monazite																									
M1A (M)	8	3202		2410	189879	2	3.43	2.0640	0.0022	0.1929	0.0002	0.94	0.07759	0.00003			1137.2	1.7	1136.9	1.5	1136.4	1.6	-0.07		
M2A (M)	10	4848		3443	201859	3	3.18	2.0609	0.0022	0.1928	0.0002	0.94	0.07753	0.00003			1136.5	1.7	1135.9	1.5	1134.9	1.6	-0.16		
M3A (M)	9	1796		1973	107315	2	5.5	2.0663	0.0022	0.1930	0.0002	0.94	0.07765	0.00003			1137.5	1.7	1137.7	1.5	1138.1	1.7	0.05		
BB0030, Z7351, Sil nodular gneiss, Kongsberg Terrane; monazite																									
M1A (M)	3	2092		411	40004	2	0.16	1.9274	0.0022	0.1842	0.0002	0.92	0.07590	0.00004			1089.7	1.8	1090.6	1.5	1092.5	1.9	0.27		
M2A (M)	7	3371		2533	184594	1	3.63	1.9312	0.0022	0.1847	0.0002	0.95	0.07585	0.00003			1092.4	1.8	1091.9	1.5	1091.1	1.6	-0.12		
M3A (M)	2	3559		3241	43097	2	4.63	1.9246	0.0021	0.1844	0.0002	0.94	0.07572	0.00003			1090.7	1.6	1089.7	1.4	1087.6	1.7	-0.31		
B99143, Z6387, Grt-Amp granodioritic gneiss, Idefjorden Terrane; titanite																									
T2B, 200 µm. 0.75	125	181		32	389	646	0.1122	1.7837	0.0083	0.1752	0.0003	0.70	0.07384	0.00028			1040.7	3.1	1039.5	6.0	1037.0	14.8	-0.4		
T1, 300 µm. 0.75A	269	189		33	435	1286	0.1011	1.7793	0.0071	0.1746	0.0003	0.71	0.07393	0.00026			1037.2	2.8	1037.9	5.2	1039.5	12.7	0.2		
T2, 200 µm. 0.75A	261	263		47	435	1753	0.0968	1.8028	0.0072	0.1759	0.0002	0.71	0.07432	0.00025			1044.7	2.7	1046.5	5.2	1050.1	12.7	0.6		
B99140, Z6386, Grt-Amp migmatitic augen gneiss, Idefjorden Terrane; titanite																									
T1, 300µm. 0.9A	351	156		27	426	1387	0.1044	1.7339	0.0072	0.1709	0.0003	0.71	0.07358	0.00026			1017.2	2.9	1021.2	5.3	1029.8	13.1	1.3		
T2, 200µm. 0.9A	279	157		27	470	1004	0.1053	1.7235	0.0074	0.1708	0.0003	0.78	0.07319	0.00034			1016.4	3.8	1017.3	5.5	1019.2	12.1	0.3		
T3, 200µm. 0.9A	155	133		24	418	544	0.1093	1.7735	0.0086	0.1739	0.0004	0.78	0.07395	0.00038			1033.7	4.3	1035.8	6.3	1040.1	13.8	0.7		
B99114, Z6382, Grt-Amp granodioritic banded gneiss, Vardefjell Shear Zone; titanite																									
T1, >200 µm. 0.75A	267	161		28	595	744	0.1535	1.6313	0.0058	0.1642	0.0003	0.79	0.07206	0.00030			980.0	3.3	982.4	4.5	987.6	9.8	0.8		
T2 , 200µm. 0.75	274	134		23	622	604	0.1389	1.6225	0.0057	0.1636	0.0003	0.81	0.07192	0.00031			976.8	3.4	979.0	4.4	983.7	9.2	0.8		
T3 , 200µm. 0.75A	332	150		26	624	817	0.1404	1.6279	0.0052	0.1640	0.0003	0.76	0.07198	0.00026			979.1	2.9	981.0	4.0	985.3	9.1	0.7		
B99111, Z6381, Grt-Amp tonalitic banded gneiss, Vardefjell Shear Zone; titanite																									
T2, 200µm. 1.0A	331	315		49	274	4035	0.0384	1.6217	0.0103	0.1632	0.0003	0.71	0.07207	0.00033			974.5	3.6	978.6	8.0	987.9	20.8	1.5		
T3, 150µm. 1.0A	332	323		49	234	4857	0.0294	1.5993	0.0121	0.1615	0.0004	0.72	0.07182	0.00039			965.1	4.3	969.9	9.5	980.9	24.9	1.7		
B99130, Z634, Grt amphibolite, Telemarkia Terrane, Telemark Sector; zircon																									
Z1, 70 µm	98	127		21	33518	4	0.0566	1.7691	0.0020	0.1722	0.0002	0.94	0.07449	0.00016			1024.5	1.7	1034.2	1.5	1054.8	1.7	3.1		
Z4, 50 µm	151	102		17	19385	8	0.0485	1.7123	0.0021	0.1696	0.0002	0.88	0.07320	0.00017			1010.2	1.8	1013.2	1.6	1019.6	2.3	1		
Z5, 50 µm	91	110		18	15714	7	0.0490	1.7040	0.0019	0.1692	0.0001	0.93	0.07303	0.00015			1007.8	1.6	1010.0	1.4	1014.8	1.8	0.7		
Z2, 50 µm	62	102		17	9919	7	0.0480	1.7067	0.0020	0.1695	0.0002	0.91	0.07301	0.00015			1009.5	1.8	1011.0	1.5	1014.3	2.1	0.5		
Z3, 50 µm	73	101		17	11286	7	0.0487	1.7072	0.0020	0.1696	0.0002	0.92	0.07299	0.00015			1010.1	1.7	1011.2	1.5	1013.6	2.0	0.4		
BB185, Amp-Cpx augen gneiss, Telemarkia Terrane, Rogaland-Vest Agder Sector; monazite																									
MTU1	2	249	87260	3939	1512	4	109.2351	1.6570	0.0038	0.1656	0.0003	0.70	0.07257	0.00012	0.04988	0.00012	988.1	3.3	992.2	2.9	1001.9	7.0	1.5	983.8	4.8
MTU2	2	526	117267	4992	2738	4	69.7304	1.4900	0.0025	0.1546	0.0002	0.88	0.06988	0.00006	0.04678	0.00012	926.7	2.8	926.3	2.1	925.0	3.4	-0.2	924.1	4.5
MTU3	3	349	82533	3522	2348	4	73.8723	1.4860	0.0031	0.1551	0.0002	0.61	0.06948	0.00012	0.04694	0.00012	929.7	2.3	924.7	2.5	913.0	7.1	-1.9	927.2	4.5
BB135, augen gneiss, Telemarkia Terrane, Rogaland-Vest Agder Sector; monazite																									
MTU1	1	2582	87323	4011	1623	21	10.5747	1.4830	0.0028	0.1539	0.0003	0.86	0.06990	0.00007	0.04667	0.00012	922.9	2.9	923.5	2.3	925.4	4.2	0.3	921.9	4.5
MTU2	1	1768	141637	6428	803	27	24.6165	1.6150	0.0027	0.1632	0.0003	0.85	0.07178	0.00006	0.04872	0.00012	974.7	2.6	976.1	2.1	979.6	3.7	0.6	961.5	4.7
MTU3	1	2383	193824	9163	4378	7	25.5071	1.6690	0.0043	0.1668	0.0004	0.83	0.07258	0.00011	0.05065	0.00013	994.5	4.5	996.8	3.3	1002.3	6.0	0.8	998.8	4.9
BB113, Amp-Cpx augen gneiss, Telemarkia Terrane, Rogaland-Vest Agder Sector; monazite																									
MTU1	2	143	55033	2292	931	3	119.9261	1.4460	0.0113	0.1524	0.0012	0.66	0.06882	0.00045	0.04606	0.00012	914.6	13.6	908.2	9.3	893.3	27.4	-2.5	910.1	8.9
MTU2	2	389	45008	1921	911	8	36.2403	1.4640	0.0054	0.1525	0.0004	0.61	0.06963	0.00021	0.04627	0.00012	914.8	5.3	915.7	4.5	917.4	12.3	0.3	914.3	4.5
BB191, Opx augen gneiss, Telemarkia Terrane, Rogaland-Vest Agder Sector; monazite																									
MTU4	2	568	53009	2487	1170	12	29.2214	1.6700	0.0035	0.1666	0.0003	0.90	0.07270	0.00007	0.05054	0.00013	993.4	3.2	997.2	2.7	1005.6	3.7	1.3	996.5	4.9
MTU5	4	173	33913	1535	1684	4	61.3339	1.6390	0.0066	0.1642	0.0006	0.95	0.07240	0.00009	0.04963	0.00012	980.0	7.2	985.3	5.0	997.1	5.0	1.8	979.1	4.8
MTU1	1	708	62607	2794	956	7	27.6220	1.5480	0.0036	0.1587	0.0004	0.46	0.07077	0.00018	0.04798	0.00012	949.4	4.7	949.7	2.8	950.9	10.4	0.2	947.3	4.6
MTU3	2	195	10328	470	538	7	16.2045	1.5740	0.0077	0.1608	0.0006	0.63	0.07102	0.00028	0.04801	0.00012	961.0	7.6	960.0	6.1	957.9	15.9	-0.4	947.8	4.6
BB649, felsic granulite, Telemarkia Terrane, Rogaland-Vest Agder Sector; monazite																									
MTU1	5	2289	53378	2724	31461	4	7.2737	1.6350	0.0028	0.1646	0.0003	0.94	0.07205	0.00004	0.04968	0.00012	982.3	2.9	983.8	2.1	987.3	2.4	0.5	980.0	4.8
MTU2	2	1239	46085	2329	3890	5	11.8248	1.6880	0.0032	0.1681	0.0003	0.86	0.07280	0.00007	0.05174	0.00013	1001.7	3.4	1004.0	2.4	1008.5	4.0	0.7	1019.6	5.0
MTU3	2	962	20951	1090	4923	3	6.8932	1.6390	0.0043	0.1643	0.0004	0.97	0.07235	0.00004	0.05031	0.00013	980.7	4.4	985.3	3.3	995.9	2.4	1.7	992.1	4.8
MTU4	5	1446	33796	1784	15572	5	7.2728	1.7210	0.0029	0.1706	0.0003	0.94	0.07317	0.00004	0.05137	0.00013	1015.4	3.0	1016.4	2.2	1018.6	2.4	0.3	1012.6	4.9
MTU5	4	1191		1523	19160	2	7.7737	1.6660	0.0028	0.1668	0.0003	0.94	0.07244	0.00004			994.7	2.5	995.7	2.2	998.4	2.4	0.4		

(1) Concentration uncertainty varies with sample weight: >10% for sample weights <10 µg, <10% for sample weights above 10 µg.
(2) Pbr = radiogenic Pb. Pbc = total common Pb in analysis corrected for spike and fractionation
(3) Atomic ratios corrected for spike, fractionation, blank and initial common Pb, except 206Pb/204Pb ratio corrected for spike and fractionation only. Errors are one sigma absolute. Pb blank: 2-5 pg for zircon and 5-10 pg for titanite; blank composition (atomic proportions): 208Pb = 0.5197; 207Pb=0.2136; 206Pb=0.2529; 204Pb = 0.0139. Common Pb correction based on Stacey-Kramers (1975) model. U blank 0.1 pg; U fractionation calculated from double spike. Pb fractionation = 0.09 ±0.03% based on SRM981.
(4) Correlation coefficient of errors in isotopic ratios
(5) Discordance of the analysis

Table 4. ID-TIMS Th-U-Pb data on monazite, zircon and titanite.

Table 5. LA-ICPMS U-Pb data on monazite

Id	$^{206}Pb/^{204}Pb$	$^{207}Pb/^{206}Pb$	±1σ (%)	$^{207}Pb/^{235}U$	±1σ (%)	$^{206}Pb/^{238}U$	±1σ (%)	R	$^{206}Pb/^{238}U$ (Ma)	±1σ	$^{207}Pb/^{206}Pb$ (Ma)	±1σ	Disc (%)
(1)	(2)	(3)		(3)		(3)		(4)	(5)		(5)		(6)
B0109, Grt-Sil metapelitic gneiss, Bamble Terrane													
01	n.t.	0.07858	0.6	2.029	1.2	0.1872	1.0	0.86	1106	11	1162	12	4.8
02	n.t.	0.07825	0.4	1.955	1.1	0.1812	1.0	0.92	1073	10	1153	8	6.9
03	n.t.	0.07758	0.6	1.924	1.2	0.1799	1.1	0.88	1066	11	1136	12	6.1
04	n.t.	0.07685	0.6	1.811	1.3	0.1709	1.2	0.90	1017	11	1117	12	9.0
05	n.t.	0.07776	0.5	1.922	1.2	0.1793	1.0	0.90	1063	10	1141	10	6.8
06	n.t.	0.07555	1.4	1.846	1.8	0.1772	1.2	0.64	1052	11	1083	28	2.9
07	n.t.	0.07911	0.6	1.999	1.2	0.1832	1.0	0.85	1085	10	1175	12	7.7
08	n.t.	0.07755	0.4	1.826	1.2	0.1707	1.2	0.94	1016	11	1135	8	10
09	n.t.	0.07724	0.6	1.998	1.2	0.1876	1.1	0.88	1108	11	1127	12	1.7
10	n.t.	0.07721	0.5	1.968	1.3	0.1848	1.2	0.91	1093	12	1127	11	3.0
11	n.t.	0.07763	0.4	2.019	1.1	0.1886	1.1	0.93	1114	11	1138	9	2.1
12	n.t.	0.07849	0.5	1.922	1.1	0.1776	1.0	0.90	1054	10	1159	10	9.1
13	n.t.	0.07767	0.5	2.044	1.1	0.1908	0.9	0.90	1126	10	1138	9	1.1
14	n.t.	0.07786	0.5	1.927	1.1	0.1795	1.0	0.92	1064	10	1143	9	6.9
15	n.t.	0.07601	1.1	1.914	2.0	0.1827	1.7	0.84	1082	17	1095	22	1.2
16	n.t.	0.07669	0.7	1.889	1.5	0.1786	1.3	0.89	1059	13	1113	13	4.8
17	n.t.	0.07595	2.0	2.013	3.9	0.1922	3.3	0.85	1133	34	1094	41	-3.6
23	17790	0.07672	0.9	2.083	1.7	0.1969	1.4	0.85	1159	15	1114	18	-4.0
24	39203	0.07639	0.7	2.156	1.8	0.2047	1.7	0.93	1201	18	1105	13	-8.6
25	28832	0.07741	1.1	1.998	2.0	0.1872	1.7	0.84	1106	17	1132	21	2.3
26	10429	0.07673	0.8	2.155	1.6	0.2037	1.4	0.85	1195	15	1114	17	-7.3
27	40294	0.07884	0.9	2.340	2.1	0.2153	1.9	0.90	1257	21	1168	18	-7.6
30	10726	0.07738	0.9	2.052	1.7	0.1923	1.5	0.86	1134	15	1131	17	-0.3
31	67878	0.07864	0.8	2.153	1.5	0.1985	1.3	0.85	1167	14	1163	16	-0.4
32	11433	0.07701	0.8	2.157	1.6	0.2031	1.3	0.84	1192	14	1122	17	-6.3
33	30793	0.07772	0.9	2.165	1.8	0.2020	1.6	0.87	1186	17	1140	17	-4.1
34	23129	0.07702	0.8	2.023	1.6	0.1905	1.4	0.85	1124	14	1122	17	-0.2
35	18604	0.07800	0.9	2.040	2.0	0.1896	1.7	0.88	1119	18	1147	18	2.4
36	6473	0.07734	1.4	2.041	2.0	0.1914	1.4	0.72	1129	15	1130	27	0.1
38	47336	0.07773	0.5	1.839	1.3	0.1716	1.2	0.91	1021	12	1140	11	10
40	68687	0.07749	0.7	1.929	1.6	0.1805	1.4	0.90	1070	14	1134	14	5.6
B0030, Sil nodular gneiss, Kongsberg Terrane													
01	25167	0.07610	1.3	2.020	2.5	0.1925	2.2	0.85	1135	22	1098	27	-3.4
02	13772	0.07680	1.8	3.204	3.4	0.3026	2.9	0.84	1704	43	1116	37	-53
03	244698	0.07742	0.8	1.940	1.9	0.1817	1.8	0.91	1076	17	1132	16	4.9
04	92401	0.07641	0.9	1.961	2.3	0.1861	2.2	0.93	1100	22	1106	18	0.5
05	25903	0.07599	1.7	1.983	3.2	0.1893	2.7	0.85	1118	28	1095	33	-2.1
06	14479	0.07611	0.9	1.841	2.2	0.1754	2.0	0.92	1042	19	1098	18	5.1
07	19821	0.07658	1.0	1.863	2.0	0.1764	1.7	0.86	1047	16	1110	20	5.7
10	30730	0.07537	0.7	1.913	2.3	0.1841	2.2	0.95	1089	22	1078	14	-1.0
12	14651	0.07567	0.9	1.890	2.1	0.1811	1.9	0.91	1073	19	1086	17	1.2
13	4033	0.07427	1.1	1.827	2.4	0.1784	2.1	0.88	1058	21	1049	23	-0.9
14	20528	0.07571	0.9	1.868	2.1	0.1789	1.9	0.90	1061	18	1087	19	2.4
B0234, Grt-Sil-Crd metapelitic gneiss, Telemarkia Terrane. Suldal Sector													
01	29450	0.07328	0.4	1.580	1.1	0.1564	1.0	0.92	936	9	1022	9	8.4
02	27659	0.07268	0.4	1.649	1.4	0.1646	1.3	0.95	982	12	1005	8	2.3
03	13050	0.07292	0.4	1.604	1.1	0.1596	1.0	0.94	954	9	1012	8	5.7
04	18138	0.07234	0.5	1.630	1.3	0.1635	1.2	0.93	976	11	996	10	2.0
05	15780	0.07343	0.5	1.617	1.2	0.1597	1.1	0.92	955	9	1026	10	6.9
06	14223	0.07217	0.5	1.575	1.1	0.1583	1.0	0.89	947	9	991	10	4.4
07	19918	0.07266	0.4	1.598	1.1	0.1595	1.0	0.93	954	9	1005	8	5.0
08	21006	0.07283	0.4	1.636	1.3	0.1629	1.2	0.95	973	11	1009	8	3.6
09	22726	0.07240	0.5	1.584	1.2	0.1587	1.1	0.91	950	9	997	10	4.8
10	19277	0.07171	0.5	1.610	1.2	0.1629	1.1	0.91	973	10	978	10	0.5
11	13815	0.07252	0.5	1.595	1.2	0.1595	1.1	0.90	954	10	1001	11	4.6
12	20537	0.07271	0.6	1.654	1.3	0.1650	1.2	0.90	984	11	1006	11	2.1
13	14255	0.07303	0.5	1.641	1.2	0.1629	1.1	0.91	973	10	1015	10	4.1
14	18624	0.07236	0.5	1.701	1.2	0.1705	1.1	0.91	1015	10	996	10	-1.9
15	8975	0.07293	0.6	1.708	1.4	0.1699	1.3	0.91	1011	12	1012	12	0.1
16	10535	0.07188	0.6	1.687	1.3	0.1702	1.2	0.89	1013	11	983	12	-3.1
17	28346	0.07242	0.5	1.652	1.1	0.1655	1.0	0.89	987	9	998	10	1.1
18	29392	0.07303	0.4	1.697	1.1	0.1685	1.0	0.93	1004	9	1015	8	1.1

(1) analysis identifier
(2) measured ratio; n.t.: ratio measured but not tabulated
(3) ratio corrected for common Pb
(4) Coefficient of correlation of errors; (5) age corrected for common Pb
(6) discordance of the analysis = 100-(100*(206Pb/238U)age/(207Pb/206Pb)age)

Table 5. LA-ICPMS U-Pb data on monazite.

Table 6. Cross-control of U-Pb analytical methods on monazite

Age		n	MSWD	Method	Lab.	Type
(Ma)		(1)				
B0109, Bamble						
1136.7	±1.4	3	1.9	ID-TIMS	GSC	Concordia age
1133	±6	12	1.4	SIMS	GSC	Concordia age
1137	±7	31	1.9	LA-ICPMS	NGU	207Pb/206Pb age
B0030, Kongsberg						
1091.7	±1.2	2		ID-TIMS	GSC	207Pb/206Pb age
1093	±6	9	1.1	SIMS	GSC	Concordia age
1095	±12	10	1.4	LA-ICPMS	NGU	207Pb/206Pb age

(1) Number of analyses

Table 6. Cross-control of U-Pb analytical methods on monazite.

Table 7. ID-NTIMS Re-Os data on molybdenite

AIRIE Run #	Locality, sample	Re, ppm	^{187}Os, ppb	Age, Ma
CT-461A	Skutterud, BU9601	29.44 ±0.10	346.1 ±1.1	1112 ±4

Assumed initial 187Os/188Os for age calculation = 0.2 ± 0.1
Absolute uncertainties shown, all at 2-sigma level
Decay constant used for 187Re is 1.666 x 10-11yr-1 (Smoliar et al. 1996)
Ages corrected for Re blank = 1.16 ± 0.024 pg, total Os = 1.9 ± 0.1 pg, 187Os/188Os = 0.24 ± 0.01

Table 7. ID-NTIMS Re-Os data on molybdenite.

One isotope dilution - negative thermal ionisation mass spectrometry (ID-NTIMS) Re-Os analysis of molybdenite was carried out at the AIRIE laboratory, Colorado State University (Table 7). Molybdenite was extracted as homogenized powder using a diamond-tipped drill. An aliquot was analysed using a Carius tube digestion, single spike isotope dilution and NTIMS measurement, according to procedures outlined in Stein et al. (2001). The model age for a single aliquot is calculated by applying the equation $^{187}Os = {}^{187}Re\ (e^{\lambda t}-1)$, where t is the age, and λ is the decay constant for ^{187}Re ($\lambda^{187}Re = 1.666\ 10^{-11}\ y^{-1}$) (Smoliar et al. 1996). The error on the Re-Os age is quoted at the 2σ level and includes propagation of all known errors, including the uncertainty surrounding the decay constant.

Pressure-temperature conditions of metamorphism were estimated in one sample. Microprobe analyses were performed using a Cameca SX100 electron microprobe equipped with 5 wave length-dispersive spectrometers (WDS) at the Institute of Geosciences, University of Oslo (Table 8). The accelerating voltage was 15 kV and the counting time 10 s on peak. The minerals were analysed at 15 nA, garnet with a focused beam, whereas biotite and plagioclase with a defocused beam (5 and 10 μm

Table 8. Microprobe chemical analyses of garnet (Grt). plagioclase (Pl). and biotite (Bt) from sample B99137

Analysis no.	#1	#18			#8	#24			#6	#23
Mineral grain	Grt 1	Grt 3			Pl 1	Pl 3			Bt 1	Bt 3
	core	core			core	core			core	core
SiO_2	37.69	37.40		Na_2O	8.46	8.30		SiO_2	35.74	35.75
TiO_2	0.01	0.02		K_2O	0.24	0.37		$Al2O_3$	18.93	17.82
Al_2O_3	21.30	21.55		SiO_2	61.38	61.58		TiO_2	3.85	4.55
Cr_2O_3	0.06	0.00		Al_2O_3	24.24	23.83		Cr_2O_3	0.04	0.05
FeO	33.35	32.80		CaO	5.75	5.47		FeO	17.34	18.06
MnO	0.77	0.72		FeO	0.02	0.02		MnO	0.00	0.05
MgO	4.16	4.45		Total	100.11	99.57		MgO	9.15	8.72
CaO	3.15	3.08		Structural formula based on 5 cations				CaO	0.00	0.00
Total	100.49	100.01		Si	2.720	2.747		Na_2O	0.04	0.16
Structral formula based on 8 cations				Al	1.266	1.253		K2O	10.09	9.97
Si	2.986	2.969		Fe	0.001	0.001		Total	95.19	95.13
Al VI	1.989	2.016		Ca	0.273	0.261		Structural formula based on 22 O		
Ti	0.001	0.001		Na	0.727	0.717		Si	5.407	5.441
Cr	0.004	0.000		K	0.014	0.021		Al	3.375	3.196
Fe^{2+}	2.210	2.177						Ti	0.438	0.521
Mn	0.052	0.049		Ab	71.7	71.8		Cr	0.005	0.005
Mg	0.491	0.526		An	26.9	26.2		Fe	2.194	2.298
Ca	0.268	0.262		Kfs	1.3	2.1		Mn	0.000	0.006
OX	11.983	11.978						Mg	2.065	1.978
								Ca	0.000	0.000
Alm	73.2	72.2						Na	0.013	0.046
Prp	16.3	17.5						K	1.948	1.936
Grs	8.9	8.7						SUM cat	15.445	15.428
Sps	1.7	1.6								
Fe/(Fe+Mg)	0.818	0.805						FeO/(FeO+MgO)	0.654	0.674

Table 8. Microprobe chemical analyses of garnet (Grt), plagioclase (Pl), and biotite (Bt) from sample B99137.

in diameter, respectively). Na and K peaks were analysed first. Standardisation is based on a selection of synthetic and natural minerals and oxides. Data reduction was done by the PAP program.

Interpretation of monazite and titanite U-Pb data

Solid-state diffusion of Pb in monazite is extremely slow (Cherniak et al. 2004). Consequently, under most crustal conditions, monazite Th-U-Pb dates record crystallization rather than diffusion processes. Abundant examples in the literature show that natural monazite commonly consists of several growth zones, each of them recording a distinct crystallization or recrystallization event, and that it is a comparatively reactive mineral in high-grade metamorphic environments in the presence of a fluid or melt (Bingen & van Breemen 1998a; Cocherie et al. 1998; Pyle & Spear 2003; Gibson et al. 2004; Williams et al. 2007). In typical pelite-psammite metasediment sequences, the bulk of metamorphic monazite appears around the sillimanite isograd and monazite coarsens in the presence of a partial melt (Smith & Barreiro 1990; Williams 2001). In typical orthogneiss, monazite generally forms in upper-amphibolite- to granulite-facies metamorphic conditions as a consequence of the breakdown of allanite, titanite and hydrous minerals (Bingen et al. 1996). Consequently, in the absence of detailed petrologic data, it is safe to state that populations of coarse-grained monazite showing comparatively simple internal zoning and collected in non-retrogressed sample suites, record at least upper amphibolite-facies metamorphism.
Solid-state diffusion of Pb is faster in titanite than in monazite (Cherniak 1993). U-Pb dates in titanite can either record (1) diffusion processes, i.e. cooling through a blocking temperature or (2) crystallization-recrystallization processes, which include neocrystallization of titanite or intracrystalline deformation by dislocation creep. A blocking temperature of c. 610°C can be derived from diffusion data by Cherniak (1993) using typical grain sizes and cooling rates (100 μm and 15 °C/my). These two lines of interpretation of titanite data have been proposed for lithologies in the Sveconorwegian belt (Bingen & van Breemen 1998a; Söderlund et al. 1999; Johansson et al. 2001).

Results

Bamble Terrane

In the core of the granulite-facies domain of Bamble, on the islands of Hisøy and Tromøy (Fig. 2), steeply dipping high-strain banded gneiss of metasedimentary origin is associated with mafic and tonalite gneiss (Knudsen et al. 1997a). Layers of metapelite and quartzite are common. Two samples of metapelitic garnet-sillimanite gneiss were collected on Hisøy (Fig. 2, samples B0109 and B0111). They contain abundant coarse-grained monazite (commonly 200-300 μm) oriented parallel to the foliation, and devoid of zoning on BSE images. Sample B0109 shows centimetre to millimetre-scale banding with layers variably enriched in garnet, sillimanite, biotite or quartz. Three ID-TIMS analyses of single monazite grains define a concordia age at 1137 ±1 Ma (Fig. 4a, Table 4), 12 SIMS U-Pb analyses in 8 monazites define a concordia age at 1133 ±6 Ma (Fig. 4b, Table 3), and 31 LA-ICPMS analyses in 17 monazites yield an average $^{207}Pb/^{206}Pb$ age of 1137 ±7 Ma (Fig. 4c, Table 5). The consistency of the data (Table 6) points to a single event of monazite growth, best estimated by the concordant ID-TIMS analyses at 1137 ±1 Ma. This foliation-parallel monazite growth is most probably coeval with the formation of the granulite-facies mineral assemblage and associated deformation leading to lithological banding. Sample B0111 contains abundant sillimanite-rich layers and garnet porphyroblasts (1-4 mm). Seven SIMS U-Pb analyses in 5 monazites yield a concordia age of 1135 ±6 Ma (Fig. 4d, Table 3).

In the amphibolite-facies domain (muscovite zone), the quartzite-rich Kragerø and Nidelva metasedimentary complexes are characterized by an assemblage of quartzite, micaceous gneiss, minor sillimanite-rich gneiss and minor orthoamphibole-cordierite rocks (Morton 1971; Starmer 1985; Nijland et al. 1993). The Nidelva Complex was sampled at Blakstad (Fig. 2). Sample B0116 is an heterogranular muscovite-bearing impure quartzite from a strongly foliated outcrop. Monazite commonly displays a core-rim structure (Fig. 3e). Four SIMS analyses performed on four cores yield a concordia age of 1134 ±14 Ma, and six analyses on five rims or crystals with homogeneous BSE contrast yield a younger concordia age at 1107 ±9 Ma (Fig. 4e, Table 3). These two ages probably reflect two separate monazite crystallization events. Sample B0024 represents the Kragerø Complex (Fig. 2). It is a comparatively weakly deformed sillimanite-bearing impure quartzite, selected from a locality showing muscovite-rich gneiss, sillimanite-bearing nodular gneiss and quartzite. The sample contains abundant tourmaline, and trace monazite and xenotime. Though monazite shows significant concentric zoning, 15 SIMS analyses in 5 crystals distributed over the different zones define a single age cluster with a concordia age at 1127 ±6 Ma (Fig. 4f, Table 3).

Kongsberg Terrane

The quartzite-rich Modum Complex in the Kongsberg Terrane is lithologically similar to the Kragerø and Nidelva Complexes in the Bamble Terrane (Starmer 1985). It includes conformable, sulfide-rich layers, commonly referred to as fahlbånd. The Skuterud cobalt mine is hosted in a muscovite-biotite-sillimanite gneiss. The ore displays an assemblage of pyrite, pyrrhotite, chalcopyrite, graphite, uraninite and cobalt minerals (Grorud 1997). It yields a Pb-Pb errorchron age of 1434 ±29 Ma (Andersen & Grorud 1998). As cobalt enrichment is directly correlated with radioactivity, Andersen and Grorud (1998) argued that this age constrains deposition of the cobalt mineralization and sets a minimun age for deposition of the sediment. Molybdenite is not a com-

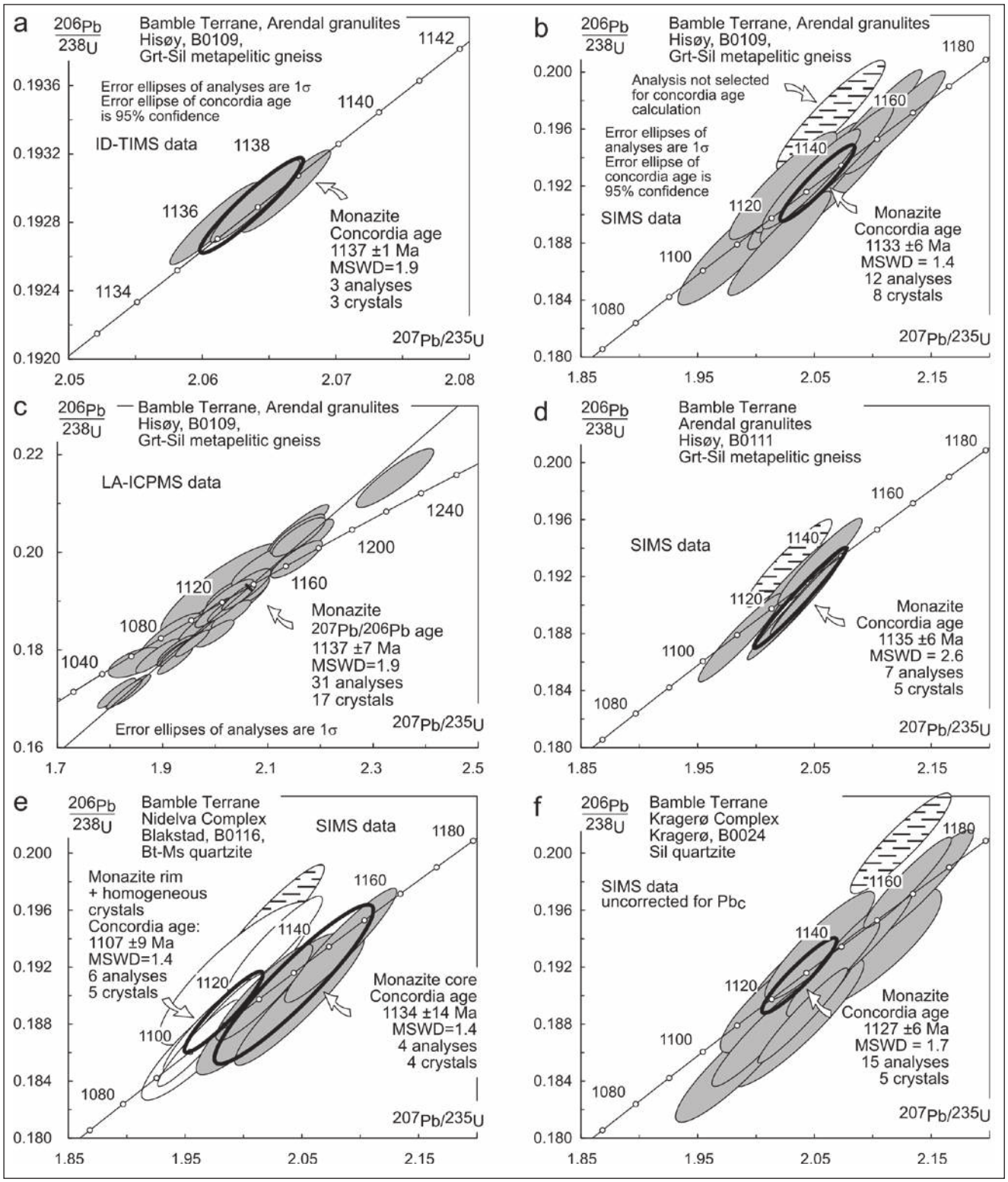

Fig. 4. Monazite U-Pb data from the Bamble Terrane. See Table 1 for abbreviation of minerals.

mon mineral at the mine. Still, sample BU9601, a float collected in the mine dump, has a few mm-size grains of molybdenite, corresponding to a whole-rock Mo content of 9 ppm. The sample shows rich impregnation of chalcopyrite, traces of pyrrhotite, and a cobalt-bearing phase in a matrix of radiating needles of gedrite with quartz and biotite. The sample is enriched in Au (2.3 ppm). Re-Os analysis of one molybdenite aggregate yields a model age of 1112 ±4 Ma (Table 7). Petrographic evidence from a variety of samples from the mine indicates that sulfide minerals were completely recrystallized during Sveconorwegian deformation (Grorud 1997). Consequently, molybdenite is regarded as a metamorphic mineral formed locally from trace Mo initially present in

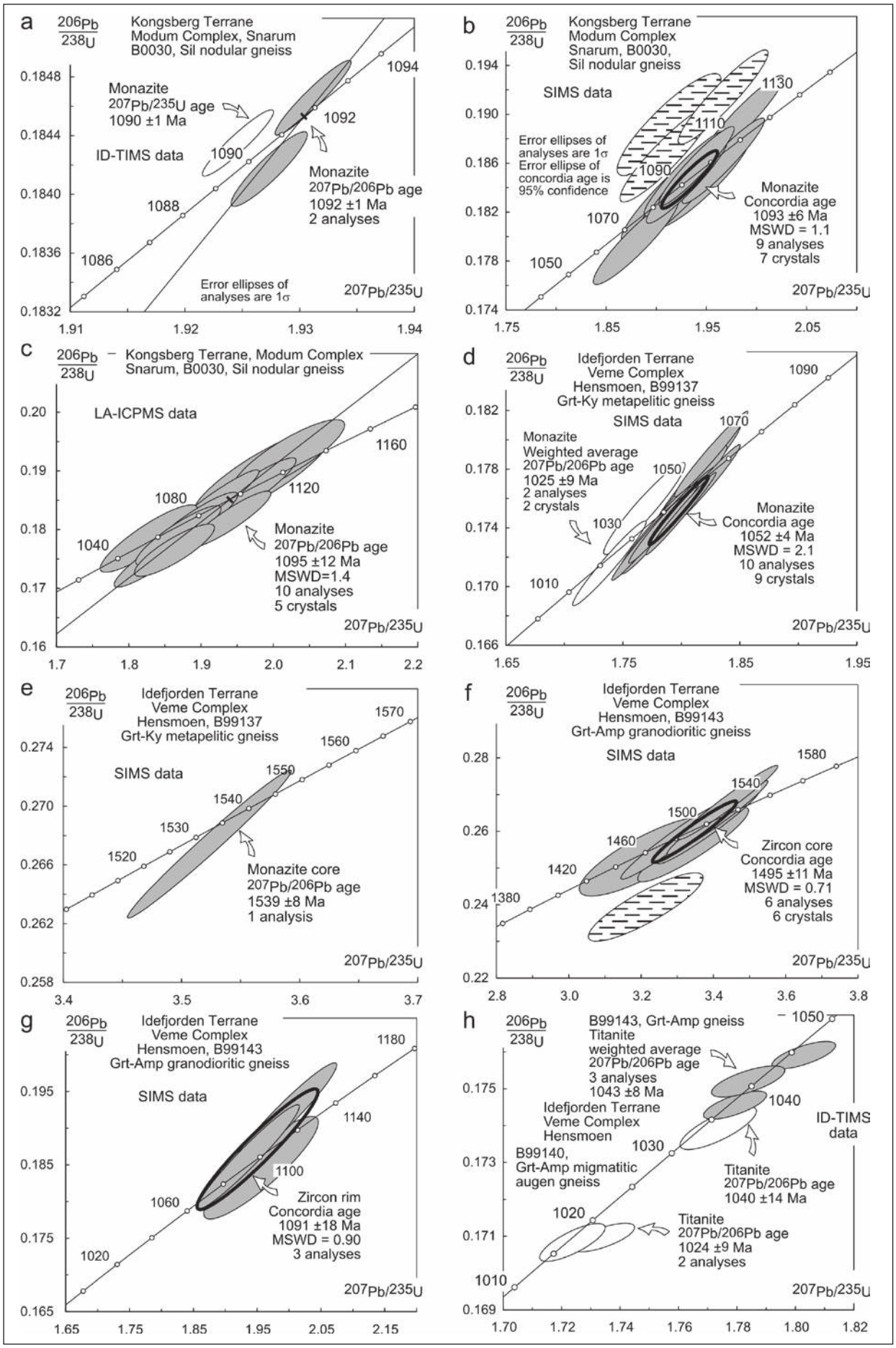

Fig. 5. Monazite, zircon and titanite U-Pb data from the Kongsberg and Idefjorden Terranes.

other minerals of the rock. The age of 1112 ±4 Ma is thus interpreted to date deformation and metamorphism in the ore body.

The Modum Complex locally contains layers of a biotite-muscovite-sillimanite gneiss with centimetre-scale oblate nodules enriched in quartz and sillimanite. A sample of such a nodular gneiss, B0030, collected some 5 km along strike from the Skuterud mine, contains abundant tourmaline, common monazite and traces of xenotime. Monazite does not appear zoned on BSE images. ID-TIMS analyses were performed on three monazite crystals. Two of them are concordant to slightly discordant and yield a $^{207}Pb/^{206}Pb$ age of 1092 ±1 Ma (Fig. 5a, Table 4). The third crystal is reversely discordant and yields a $^{207}Pb/^{235}U$ age of 1090 ±1 Ma and a $^{207}Pb/^{206}Pb$ age of 1088 ±2 Ma suggesting that the monazite population of this sample may not be strictly homogeneous or that the $^{206}Pb/^{238}U$ age of some grains is affected by intermediate-daughter disequilibrium (Schärer 1984). Nine out of twelve SIMS analyses in seven monazite crystals are concordant and define a concordia age at 1093 ±6 Ma (Fig. 5b, Table 3). The three remaining SIMS analyses are reversely discordant, and also suggest significant heterogeneity in the monazite population. Ten LA-ICPMS analyses in 5 monazite crystals give a $^{207}Pb/^{206}Pb$ age of 1095 ±12 Ma (Fig. 5c, Table 5). The ID-TIMS, SIMS and LA-ICPMS age estimates overlap (Table 6). The ID-TIMS age of 1092 ±1 Ma is the most precise one and is interpreted to date crystallization of monazite together with the development of the amphibolite-facies sillimanite-bearing mineral assemblage.

Idefjorden Terrane, west of Oslo rift

West of the Oslo rift, the Idefjorden Terrane contains a metagreywacke-rich metasupracrustal sequence, referred to as the Veme Complex (Fig. 2) (Bingen et al. 2001b). At Hensmoen, a southwest-dipping sequence of variably banded and variably foliated ortho- and paragneisses is characterized by pervasive amphibolite-facies garnet blastesis. Garnet is present in all lithologies. It has generally a rounded habit and predates the last deformation phase recorded in this section. Three samples represent three main lithologies along this c. 2 km section: a metapelitic gneiss (B99137), a granodioritic gneiss (B99143) and an augen gneiss (B99140).

Sample B99137, is a kyanite-bearing metapelite layer hosted in a migmatitic banded gneiss. The sample contains an equilibrium assemblage of garnet, biotite, K-feldspar, plagioclase, kyanite, rutile and quartz attesting to high-pressure amphibolite-facies conditions. No retrogression of this assemblage is detected. Pressure-temperature conditions were estimated using the garnet-kyanite-plagioclase-quartz (GASP) barometer calibrated by Holland and Powell (1998), and the garnet-biotite thermometer. For the garnet-biotite thermometer, three calibrations by Perchuk et al. (1985), Krogh et al. (1990) and Kaneko and Miyano (2004) were used. Similar pressure-temperature estimates were derived from four sets of mineral analyses representing equilibrium microdomains. The highest estimates from one of these, range from 1.00 GPa-688 °C to 1.17 GPa-780 °C, depending on the selected calibration of the garnet-biotite thermometer (Fig. 6). Sample B99137 contains abundant monazite, showing weak internal BSE contrast. Ten out of 15 SIMS analyses from nine monazite crystals define a tight concordant cluster with a concordia age at 1052 ±4 Ma (Fig. 5g, Table 3). This age is interpreted to be the age of crystallization of the main population of coarse-grained monazite belonging to the kyanite-bearing assemblage (1.00-1.17 GPa, 688-780 °C). Two analyses in two crystals give a distinctly younger age of 1025 ±9 Ma (weighted average $^{207}Pb/^{206}Pb$ age), interpreted as monazite crystallization after peak metamorphism. One of the rarely detected cores yields a concordant age at 1539 ±8 Ma (Fig. 5e, Table 3). If interpreted as metamorphic, this monazite age is evidence for a Gothian metamorphism, and implies that sedimentation now represented by the paragneiss sequence exposed at Hensmoen took place before 1540 Ma.

Sample B99143 is an amphibole-garnet-biotite-allanite-bearing granodioritic gneiss (SiO_2 =64.9 %, K_2O =4.4 %), collected in a homogeneous outcrop. It probably represents an orthogneiss sheet in the sequence. Zircon cores with magmatic oscillatory zoning define a concordia age at 1495 ±11 Ma (6 SIMS analyses in 6 cores, Fig. 5f, Table 2), and date magmatic intrusion of a granodioritic protolith. Uranium-rich (450–550 ppm) metamorphic zircon rims are locally present (Fig. 3a). Three SIMS analyses, collected with a 12 μm beam from three rims,

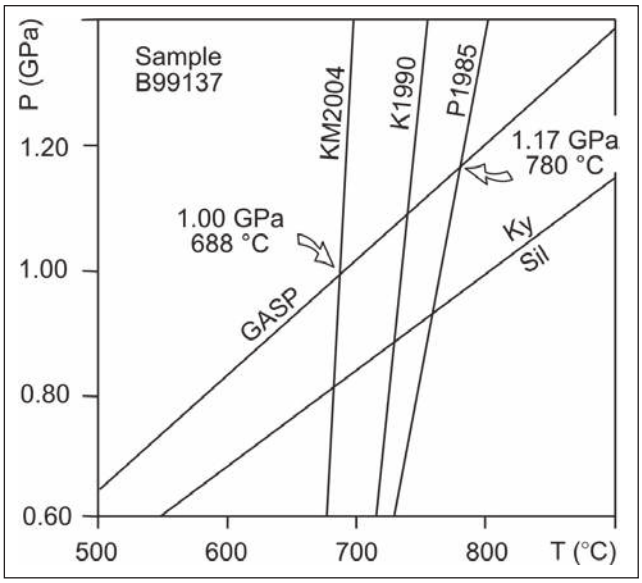

Fig. 6. Pressure-temperature diagram showing thermobarometric calculation for garnet-kyanite metapelitic gneiss B99137, Idefjorden Terrane, Hensmoen locality. GASP: garnet-kyanite-plagioclase-quartz barometer following Holland & Powell (1998). Garnet-biotite thermometer: P1985: calibrations by Perchuk et al. (1985); K1990: Krogh et al. (1990); KM2004: Kaneko and Miyano (2004). Intersection of Keq lines gives P-T estimates of 1.00 GPa-688 °C to 1.17 GPa-780 °C.

yield a concordia age at 1091 ±18 Ma (Fig. 5g). Sample B99143 was collected close to an outcrop of sillimanite-bearing (kyanite-free) metapelitic gneiss, showing abundant inclusions of sillimanite inside garnet phenoblasts. This association suggests that the metamorphism dated at 1091 ±18 Ma was in the sillimanite stability field, and took place before kyanite-grade metamorphism recorded in sample B99137 (1052 ±4 Ma). Sample B99143 contains abundant amber titanite forming oblate discs aligned parallel to the fabric of the gneiss. Three titanite fractions define a $^{207}Pb/^{206}Pb$ age of 1043 ±8 Ma (Fig. 5h; Table 4).

Sample B99140 was collected some 300 m from sample B99143 in a garnet-bearing augen gneiss with conspicuous cm-scale leucosome pods. Sample B99140 is richer in biotite than B99143. One titanite fraction has a $^{207}Pb/^{206}Pb$ age of 1040 ±14 Ma, and two fractions, with similar characteristics, define an age of 1024 ±9 Ma (Fig. 5h; Table 4).

Vardefjell Shear Zone and Telemarkia hanging wall

The Vardefjell Shear Zone represents the boundary between the Telemarkia and Idefjorden Terranes (Fig. 2). It trends NW-SE and dips to the southwest (20–50°). It is characterized by amphibolite-facies banded gneiss rich in amphibolite layers and 1 to 50 m thick amphibolite boudins. Metamorphic garnet is common in both the banded gneiss and amphibolite boudins. The shear zone is cut by numerous undeformed pegmatite dykes, probably related to intrusion of the nearby unfoliated Flå granite pluton (Fig. 2). The hanging wall of the shear zone in the Telemark Sector is referred to as the Hallingdal Complex (Bingen et al. 2001b) Here, the metamorphic grade decreases progressively towards the southwest.

Two samples of amphibole-bearing banded gneiss were collected in the centre of the Vardefjell Shear Zone in the Flå area. They show a strong planar gneissic fabric and mm-scale quartz ribbons. Sample B99111 was affected by grain-size reduction during shearing (mylonitization), as is evident from the occurrence of 3 to 6 mm large plagioclase and amphibole porphyroclasts hosted in a granoblastic matrix. This sample is granodioritic to tonalitic in composition (SiO_2 =63.6 %, K_2O =0.9 %) and interpreted as a sheared orthogneiss. The sample contains zircons with a core-rim structure (Fig. 3b, c). A core is present in almost every crystal. The core is oscillatory zoned and has a typical magmatic morphology. The rim is rich in uranium (260-740 ppm) and poor in Th (<10 ppm) and interpreted as metamorphic. A few rounded crystals without visible core, but mainly made up of U-rich Th-poor zircon with a faint sector zoning (Fig. 3c), are also interpreted as metamorphic. Seven SIMS analyses in seven cores define a concordia age of 1528 ±16 Ma (Fig. 7a, Table 2). This age is interpreted to record the intrusion of the magmatic protolith. Three zircon cores ranging from 1626 ±31 to 1575 ±18 Ma (near-concordant analyses) may be inherited from the source of the rock. Fifteen analyses of metamorphic zircon define a concordia age at 1012 ±7 Ma (Fig. 7b, Table 2) and date an amphibolite-facies metamorphic overprint. It also represents a maximum age for the mylonitic fabric observed in this sample, as grain-size reduction post-dates peak metamorphic conditions.

Sample B99114 is granodioritic to granitic in composition (SiO_2 =70.6 %, K_2O =4.6 %). It contains small zircons with a core-rim structure. The cores are oscillatory zoned while narrow Th-poor (<5 ppm) rims are generally located at the tip of crystals (Fig. 3d). Seven out of eight SIMS analyses in the core define a concordia age of 1507 ±14 Ma reflecting magmatic intrusion age of the granodioritic protolith (Fig. 7c, Table 2). Six SIMS analyses in the rim yield a concordia age at 1008 ±14 Ma (Fig. 7d, Table 2). The two gneiss samples contain oblate, amber coloured titanite aligned in the planar fabric. In sample B99114, three titanite fractions are nearly concordant. In sample B99111, two fractions are more discordant and less radiogenic (230 <$^{206}Pb/^{204}Pb$ <280). Together, the five fractions define a weighted average $^{207}Pb/^{206}Pb$ age of 985 ±5 Ma (Fig. 7e, Table 4).

In the Hallingdal complex, in the Telemarkia hanging wall, a garnet-bearing amphibolite boudin, about 50 m thick, was sampled. The boudin is weakly deformed and contains conspicuous cm-thick leucosome pockets. Sample B99130 shows a well-equilibrated garnet-bearing metamorphic texture. It is rich in biotite and characterized by small (<100 μm) rounded zircons, with a typical metamorphic habit. Five zircon fractions were analysed by ID-TIMS. Three of them overlap and are nearly concordant. They yield a weighted average $^{207}Pb/^{206}Pb$ age of 1014 ±1 Ma (Fig. 7f, Table 4). The two other fractions are more discordant and contain an inherited component older than 1014 Ma. The age of 1014 ±1 Ma is interpreted as the age of crystallization of metamorphic zircon. Metamorphic zircon in migmatitic amphibolite may crystallize as a consequence of release of Zr during conversion of the magmatic assemblage into a metamorphic one, or may be related to the formation of leucosome pockets (Bussy et al. 1995; Fraser et al. 1997; Bingen et al. 2001a).

Telemarkia Terrane, Suldal Sector

To the west of the Mandal-Ustaoset Fault and Shear Zone, in the Suldal Sector, metasupracrustal rocks of andesite-dacite composition contain minor staurolite-grade pelitic layers (Grjotdokki-Nesflaten supracrustal rocks, Bykle area, Fig. 2). These supracrustal rocks are surrounded by an amphibolite-facies gneiss complex, called the Botsvatn Complex (Sigmond 1978). The Botsvatn Complex is made up of banded gneiss and c. 1500 Ma felsic orthogneiss (Bingen et al. 2005). The contact between the metasupracrustal rocks and the Botsvatn Complex is parallel to a strong planar deformation fabric. No unconformity can be observed at the base of the metasupracrustal rocks. Sample B0234, collected at Rygnestad (Fig. 2), is a pelitic layer in a banded gneiss of the Botsvatn Complex. Centimetre-scale leucosomes are present. Sample

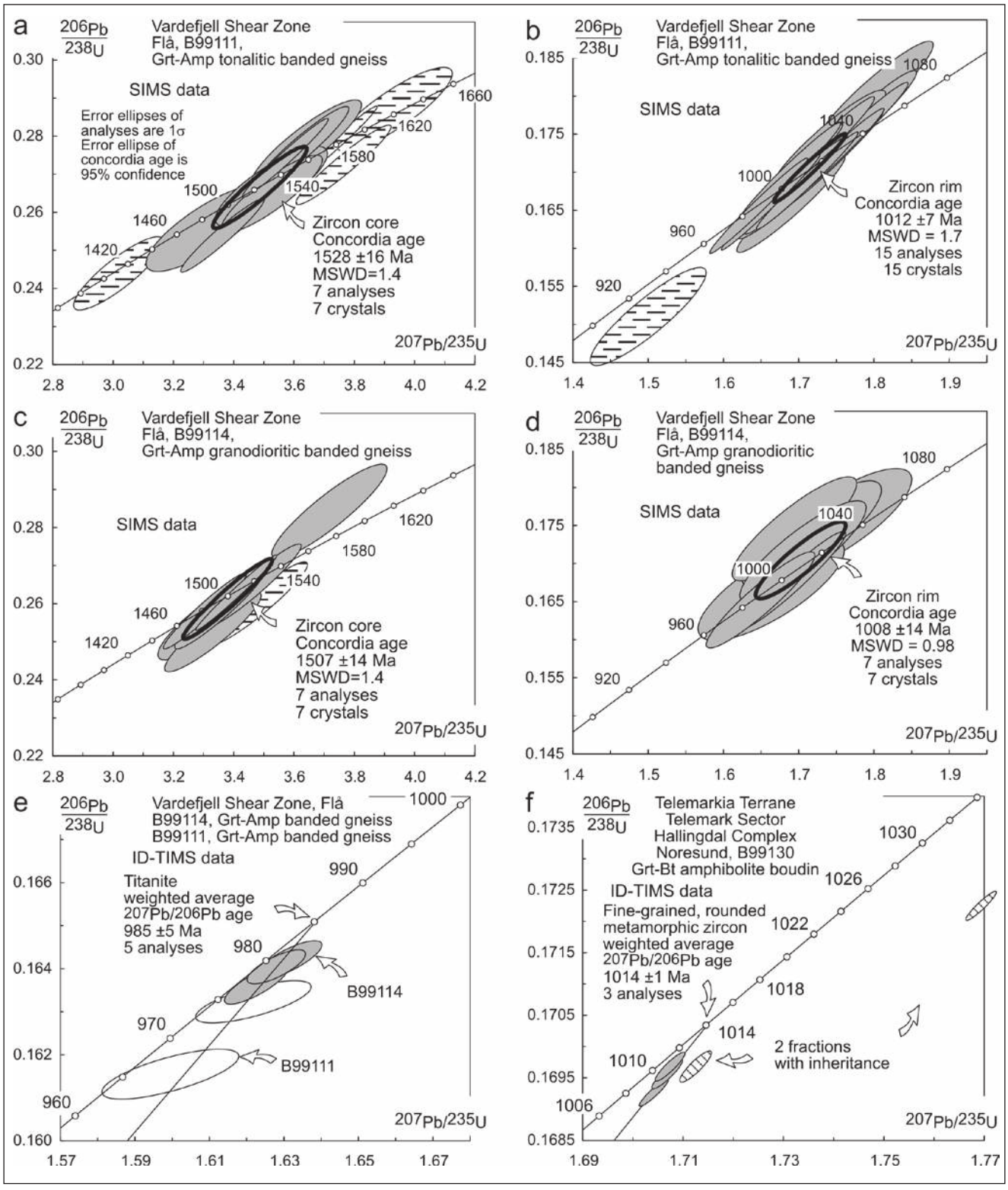

Fig. 7. Zircon and titanite U-Pb data from the Vardefjell Shear Zone.

B0234 contains porphyroblasts of garnet in a biotite-sillimanite-garnet-plagioclase-bearing matrix. Cordierite (now retrogressed to pinite) commonly surrounds garnet porphyroblasts, and is interpreted to be the product of a decompression reaction. Coarse-grained (commonly >200 μm) monazite is abundant and occurs in both the matrix and garnet porphyroblasts. Monazite is generally not zoned on BSE images. Eighteen analyses, performed with LA-ICPMS, define a weighted average $^{207}Pb/^{206}Pb$ age of 1005 ±7 Ma (Fig. 8a, Table 5). This age records monazite growth, most probably during partial melting and the formation of the sillimanite-garnet assemblage. The data demonstrate a Sveconorwegian age for amphibolite-facies metamorphism in the Botsvatn Complex.

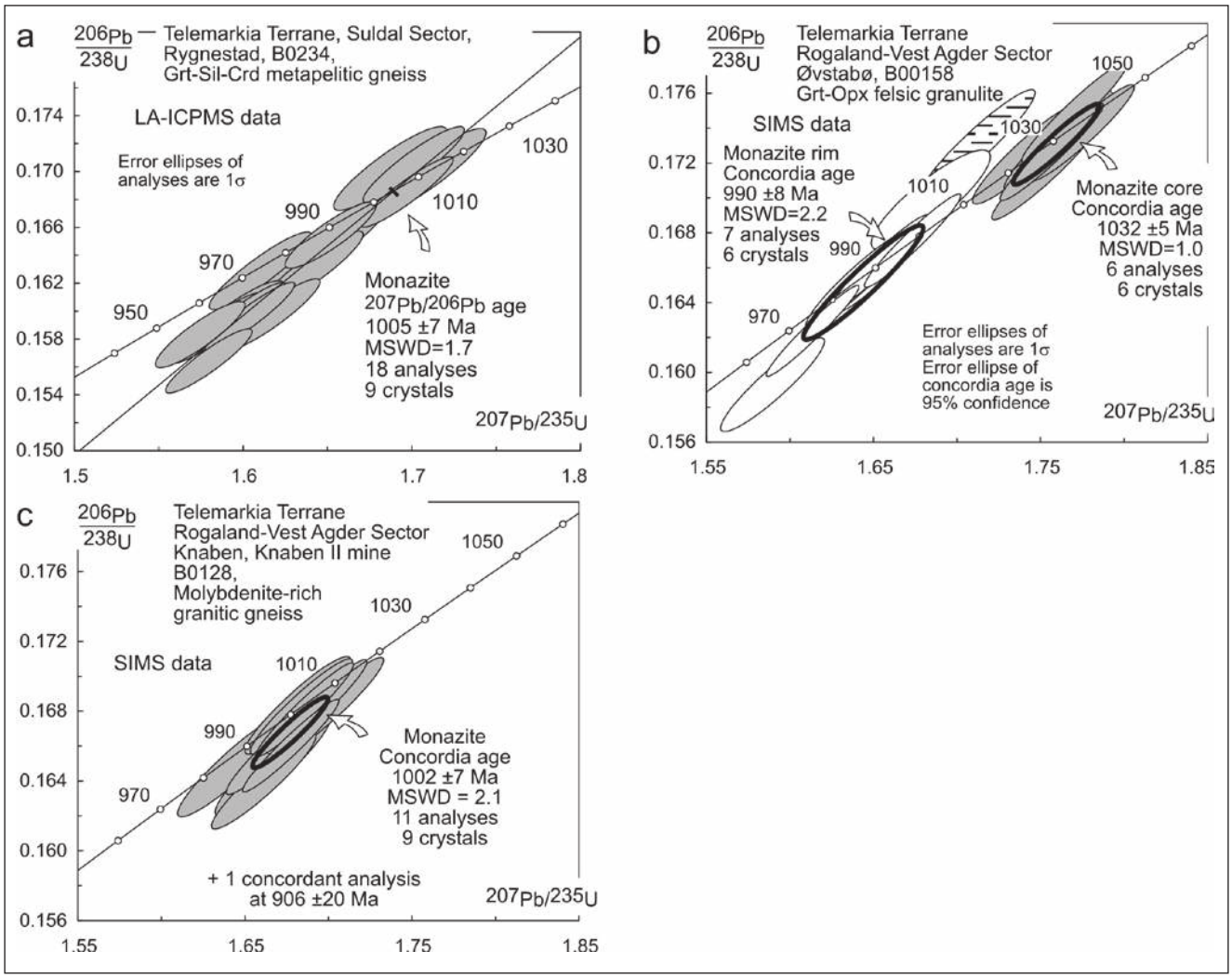

Fig. 8. Monazite U-Pb data from the Suldal and Rogaland-Vest Agder Sectors, Telemarkia Terrane.

Telemarkia Terrane, Rogaland-Vest Agder Sector

In the Rogaland-Vest Agder Sector, published monazite ID-TIMS U-Pb data from 11 samples distributed in the amphibolite- and granulite-facies domains range from 1024 ±1 to 904 ±5 Ma (Bingen & van Breemen 1998a). In the granulite-facies domain, no apparent time gap is recorded during this 120 m.y. time span in the monazite data set. The question arises as to whether this age pattern reflects (1) continuous crystallization of monazite, or (2) a mixture of domains with ages corresponding to the M1 and M2 metamorphic events, as defined by petrology in this sector (Tobi et al. 1985). The most common way of handling composite monazite grains is to use microanalytical methods, like SIMS, electron microprobe, or LA-ICPMS. In order to complement the available ID-TIMS data set, and preserve full advantage of the precision of this method, an alternative way is used here. It consists of collecting paired U-Pb and Th-Pb data on single monazite grains with the ID-TIMS method (Table 4). Th and U contents are not directly correlated in monazite. Composite monazite crystals made up of domains with distinct ages and distinct Th/U ratios will provide distinct apparent U-Pb and Th-Pb ages. A simple calculation, using typical values for the situation under consideration here, shows that the apparent $^{208}Pb/^{232}Th$ age of a monazite made up of two age domains at 1000 and 900 Ma, 50 % volume each, will decrease by c. 17 m.y. by doubling the Th content in the 900 Ma domain, relative to a grain with homogeneously distributed Th and U. This calculation suggests that analyses characterized by significant differences between the apparent $^{208}Pb/^{232}Th$ and $^{207}Pb/^{235}U$ ages may be derived from composite monazite grains. The $^{206}Pb/^{238}U$ age can be affected by intermediate-daughter disequilibrium and is thus regarded as less reliable than the $^{207}Pb/^{235}U$ age for defining the crystallization age of a monazite (Schärer 1984).

Paired U-Pb and Th-Pb data were collected on monazite from five of the samples investigated by Bingen and van Breemen (1998a) (Fig. 2, Table 4). Samples B113 and B185 are hornblende-clinopyroxene augen gneisses collected in the amphibolite-facies domain to the west of the clinopyroxene isograd. Sample B135 is a biotite augen gneiss from the same zone. Sample B191 is also a biotite augen gneiss collected in the granulite-facies domain

close to the contact with the Rogaland AMC Complex. Sample B649 is an anhydrous (biotite-free) charnockitic gneiss collected to the west of the pigeonite isograd. With few exceptions, BSE images of monazite crystals from these samples show no visible zoning. Sixteen analyses are nearly concordant for the U-Pb system (+1.8 to -2.5% discordance) suggesting that no significant loss of radiogenic Pb occurred after crystallization. Five analyses have distinct $^{207}Pb/^{235}U$ and $^{208}Pb/^{232}Th$ ages. These have apparent $^{208}Pb/^{232}Th$ ages older than 950 Ma, suggesting these monazite crystals are composite and consist of a M1 core surrounded by a variably thick M2 rim. Eleven analyses yield equivalent $^{208}Pb/^{232}Th$, $^{207}Pb/^{235}U$ and $^{206}Pb/^{238}U$ ages (Fig. 9). Accordingly, it cannot be demonstrated that these crysals consist of more than one age domain, within resolution of the analytical method. In the three amphibolite-facies samples, six of these crystals define three $^{208}Pb/^{232}Th$ ages or age ranges, at 999 ±5, 927 to 922 ±5, and 914 to 910 ±5 Ma. In the two granulite-facies samples, five crystals define four $^{208}Pb/^{232}Th$ ages at 1013 ±5, 997 ±5, 980 to 979 ±5, and 947 ±5 Ma (Fig. 9a). These results suggest, but do not demonstrate, crystallization of more than two generations of monazite in Rogaland-Vest Agder, including a minor population of monazite at 947 ±5 Ma, midway between the M1 and M2 metamorphic events.

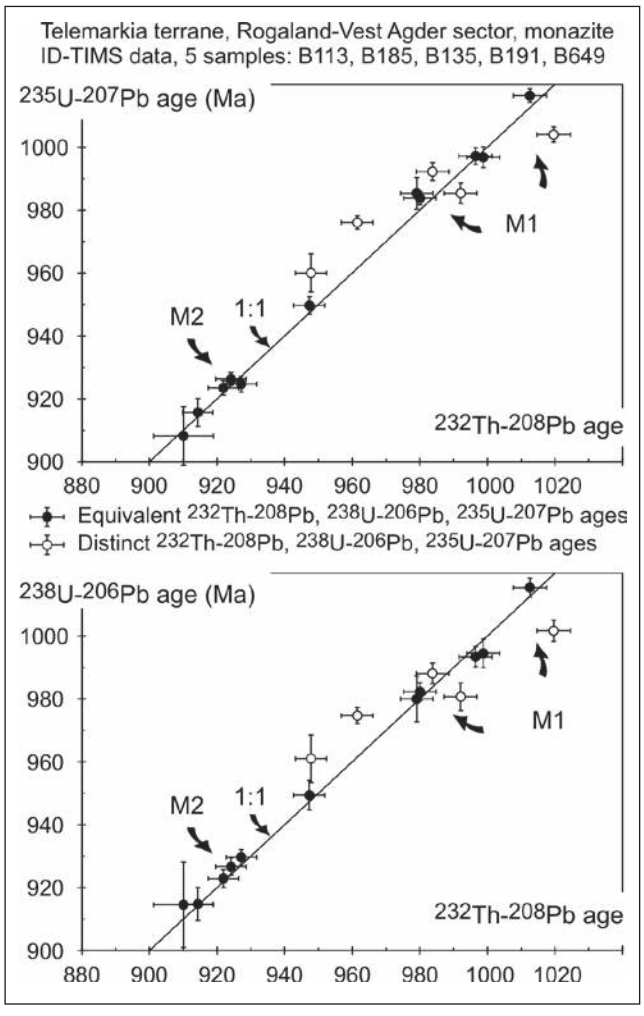

Fig. 9. Paired Th-Pb and U-Pb ID-TIMS data on monazite from the Rogaland-Vest Agder Sector.

The geochronology of M1 regional metamorphism is also investigated with SIMS using two samples collected more than 30 km away from the contact of the Rogaland AMC complex, presumably outside of the area affected by M2 metamorphism. Sample B00158 is a felsic orthopyroxene-garnet-biotite paragneiss from a lithologically homogeneous outcrop at Øvstabø (Fig. 2). The sample has a granulite-facies assemblage, though collected some 10 km to the east of the orthopyroxene isograd, as mapped by Tobi et al. (1985). The sample contains abundant coarse-grained monazite (commonly >200 μm) with a conspicuous core-rim structure (Fig. 3f). The rim is volumetrically minor and forms embayments into the core. It is enriched in thorium. Six SIMS analyses from the cores of six monazites yield a concordia age at 1032 ±5 Ma, while seven analyses from the rims yield a distinctly younger concordia age at 990 ±8 Ma (Fig. 8b, Table 3). Garnet from the coarse-grained orthopyroxene-garnet-biotite assemblage is locally overgrown by a rim of garnet + quartz. Locally, the biotite is apparently breaking down and intergrown with quartz and plagioclase. These petrographic relationships suggest that a local interstitial melt was present after formation of the main coarse-grained granulite-facies assemblage and resulted in the formation of the garnet rim. They also suggest, but do not demonstrate, that the voluminous 1032 ±5 Ma monazite core is coeval with the coarse-grained granulite-facies assemblage and that the 990 ±8 Ma rim is coeval with formation of the garnet rim.

In the Knaben area (Fig. 2), molybdenum mineralizations are hosted in a N-S trending amphibolite-facies banded gneiss, known as the Knaben gneiss. Sample B0128 represents the main ore body at the Knaben II mine. It is made up of a leucocratic molybdenite-rich biotite-granitic gneiss. Monazite forms crystals smaller than 200 μm, and these are commonly zoned on BSE images. Eleven SIMS analyses in 9 monazite crystals yield a concordia age at 1002 ±7 Ma (Fig. 8c, Table 3). Monazite growth probably took place during the prominent hydrothermal ore-forming event observed at this locality. One monazite crystal yields a distinctly younger age at 906 ±20 Ma.

Discussion

Bamble and Kongsberg Terranes

The early Sveconorwegian age of granulite-facies metamorphism in the Bamble Terrane was established by Kullerud and Dahlgren (1993), on the basis of Sm-Nd mineral isochrons, the best of which gave an age of 1098 ±7 Ma. A whole-rock Pb-Pb correlation line, based on paragneiss samples from the Kongsberg and Bamble Terranes, gave an age of 1131 ±30 Ma (Andersen & Munz 1995). This line, though difficult to interpret in detail,

underscores the regional significance of Sveconorwegian overprint in these terranes. Recent geochronological data indicate the presence of two metamorphic events, a first event at 1140-1125 Ma restricted to Bamble and a second one at 1110-1080 Ma recorded in both terranes (Fig. 10).

The first phase at 1140-1125 Ma is recorded by a few published ages from the granulite-facies domain in the Arendal area. It includes a monazite ID-TIMS analysis at 1145 ±3 Ma from a metapelitic gneiss (Cosca et al. 1998), SIMS analyses of metamorphic zircon in two samples at 1125 ±46 and 1124 ±8 Ma (Knudsen et al. 1997b; Knudsen & Andersen 1999), and a titanite date at 1137 ±2 Ma from a marble collected on Tromøy (Cosca et al. 1998; Fig. 10). New monazite data in four samples (Fig. 4) provide a narrower age bracket extending from 1137 ±1 to 1127 ±6 Ma for this event, and show that it is present in both the amphibolite-facies domain (samples B0116, B0024) and the granulite-facies domain (samples B0109, B0111, Fig. 2). Monazite in the two granulite-facies samples probably dates the sillimanite-bearing granulite-facies assemblage, and provides an estimate for peak intermediate-pressure granulite-facies metamorphism (0.70 ±0.11 GPa).

The second event at 1110-1080 Ma is recorded in the Bamble Terrane by a monazite date at 1107 ±9 Ma in the amphibolite-facies domain (sample B0116, Fig. 4e), and titanite dates between 1106 ±2 and 1091 ±2 Ma in four samples located in the amphibolite-facies domain and marginal zone of the granulite-facies domain (Cosca et al. 1998; de Haas et al. 2002; Fig. 10). The monazite and titanite data overlap with the main cluster of amphibole $^{40}Ar/^{39}Ar$ plateau ages, between 1099 ±3 and 1079 ±5 Ma (18 samples, average value at 1089 ±3 Ma), being from samples taken from the amphibolite- and granulite-facies domains (Cosca & O'Nions 1994; Cosca et al. 1998).

Estimates of the timing of amphibolite-facies metamorphism in the Kongsberg Terrane are restricted to the Modum Complex. They include a SIMS U-Pb age of 1102 ±28 Ma for zircon rims in a quartzite (Bingen et al., 2001), the molybdenite age at 1112 ±4 Ma from the Skuterud mine (Table 7) and the monazite age from a nearby nodular gneiss at 1092 ±1 Ma (Fig. 5a). These two last ages are distinct, even if uncertainty regarding decay constants is propagated for calculation of both the Re-Os and U-Pb systems (1112 ±4 Ma vs. 1092 ±5 Ma). The data may suggest that sulfide minerals in the Skuterud

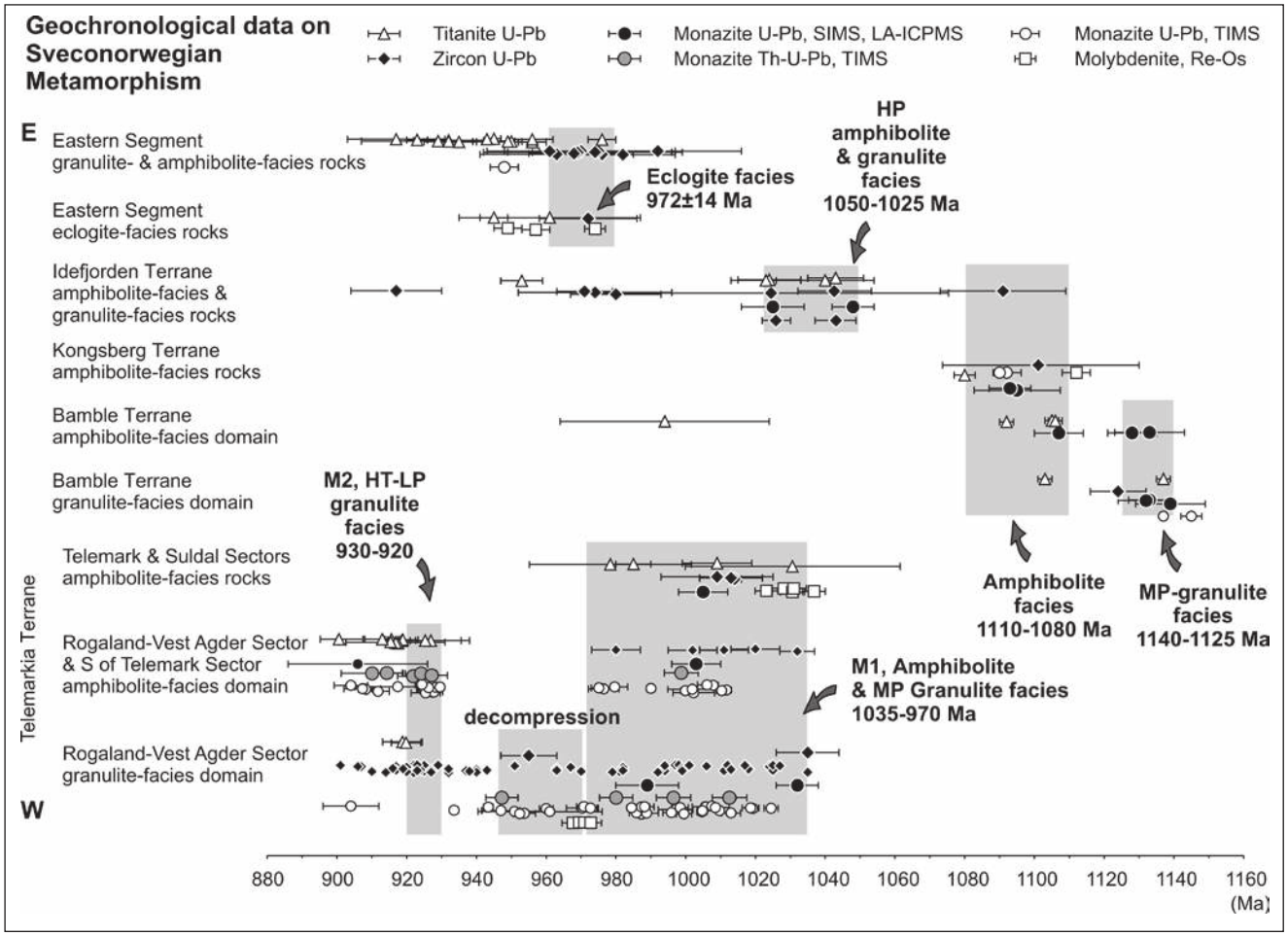

Fig. 10. Summary of published geochronological data on metamorphism in the lithotectonic units and main shear zones of the Sveconorwegian belt. The data are presented from East (top) to west (bottom). Data and source of data are listed in the text.

ore body were overprinted during the prograde part of metamorphism leading to crystallization of molybdenite at 1112 ±4 Ma, while formation of monazite in the wallrock took place during peak sillimanite-grade metamorphism, slightly later, at 1092 ±1 Ma. A titanite date from an albitite constrains hydrothermal activity after peak metamorphism at 1080 ±3 Ma (Munz et al. 1994; Fig. 10).

The distribution of data on the Bamble and Kongsberg Terranes (Fig. 10) suggests that the 1110-1080 Ma event includes the peak of amphibolite-facies metamorphism in the Kongsberg Terrane, while in the Bamble Terrane, it corresponds to a post-peak phase of regional cooling and unroofing, as provided by interpretation of amphibole $^{40}Ar/^{39}Ar$ plateau ages (Cosca et al. 1998). The recording of both events in monazite from one sample located in the amphibolite-facies domain in Bamble (B01016, Fig. 4e) indicates that the two events affected the same rocks, rather than two distinct tectonic slivers.

The 1140-1080 Ma metamorphic events are associated with widespread lithological banding and isoclinal folding, and resulted in the prominent structural grain, trending NE–SW in the Bamble Terrane and N-S in the Kongsberg Terrane (Starmer 1985). Isoclinal folding in Bamble is largely related to northwest-directed shortening (Henderson & Ihlen 2004). Northwestwards thrusting along the Kristiansand-Porsgrunn Shear Zone represents a late increment of this deformation (Henderson & Ihlen 2004).
No significant metamorphic event younger than 1080 Ma is recorded in the Bamble and Kongsberg Terranes, except in the vicinity of the Kristiansand-Porsgrunn Shear Zone, where secondary titanite is dated at 994 ±30 Ma (de Haas et al. 2002; Fig. 10). $^{40}Ar/^{39}Ar$ data on muscovite porphyroblasts constrain the timing of a phase of extensional deformation along the shear zone to be between 891 ±3 and 880 ±3 Ma (Mulch et al. 2005).

Idefjorden Terrane

The Idefjorden Terrane bears evidence of two tectonometamorphic events, the Gothian and Sveconorwegian. Sveconorwegian deformation and metamorphism are not everywhere penetrative. For example, in the east of the terrane, Mesoproterozoic supracrustal rocks are not affected by high-grade metamorphism and still show well-preserved primary volcanic features (Åmal area; Lundqvist & Skiöld 1993). In the west of the terrane, primary Bouma sequences are locally preserved in turbiditic metasandstone of the Stora Le-Marstrand Formation and Veme Complex (Brewer et al. 1998; Bingen et al. 2001b). Also in the west of the terrane, a 1555 ±2 Ma dyke is shown to cut an amphibolite-facies fabric, demonstrating both Gothian high-grade metamorphism and lack of Sveconorwegian deformation (Burö locality, Connelly & Åhäll 1996).

The timing of Gothian amphibolite-facies metamorphism is estimated by U-Pb data on metamorphic zircon rims at 1540 ±32 and 1540 ±7 Ma in two samples of paragneiss east of the Oslo rift (Nord-Koster psammite and Burnholmen migmatite, Åhäll & Connelly 2008) and on a monazite core at 1539 ±8 Ma in a metapelitic gneiss (sample BB99137, Fig. 5e) west of the Oslo rift.

The general, orogen-parallel, N-S to NW-SE structural trend in the Idefjorden Terrane and the shear zones parallel to this trend (Fig. 1), are undoubtedly Sveconorwegian in age. Mafic dykes with a high-pressure granulite-facies overprint are locally reported in the eastern part of the terrane, east of the Göta Älv Shear Zone (Trollhättan locality; Söderlund et al. 2008). Pressure-temperature conditions range from c. 1.5 GPa, 740 °C to c. 1.0 GPa, 700 °C. The timing of this metamorphism is estimated by means of U-Pb, Sm-Nd and Lu-Hf data to be between 1046 ±6 and 1026 ±4 Ma (Söderlund et al. 2008, Fig. 10). Amphibolite-facies metamorphism west of the Göta Älv Shear Zone and Dalsland Boundary Zone is dated at 1043 ±11 Ma and 1024 ±52 Ma by zircon data and c. 1023 Ma by titanite data (Hansen et al. 1989; Åhäll et al. 1998; Austin Hegardt et al. 2007) (Fig. 10).

West of the Oslo rift, zircon, monazite and titanite U-Pb data reported in this study from the Hensmoen locality, define three age groups probably corresponding to three metamorphic events (Fig. 5, 10). The first group includes a few zircon rims at 1091 ±18 Ma in one orthogneiss sample (B99143), and presumably records amphibolite-facies metamorphism in the sillimanite stability field. The evidence for this metamorphic event is comparatively weak today, but cannot be entirely neglected. The second group corresponds to monazite at 1052 ±4 Ma in one kyanite-bearing metapelitic gneiss sample (BB99137) and titanite at 1043 ±8 - 1040 ±14 Ma in two samples (BB99143-140). The third group, arguably distinct from the second one, corresponds to a minor population of monazite in one sample at 1025 ±9 Ma (BB99137), and to titanite in one sample at 1024 ±9 Ma (B99140). The coarse-grained monazite population at 1052 ±4 Ma probably reflects peak high-pressure amphibolite-facies metamorphism (kyanite stability field, 1.00-1.17 GPa, 688-780 °C). The young group at c. 1025 Ma possibly records local decompression partial melting, as it is recorded in a leucosome-bearing sample. Available titanite apparent ages pertain to the second and third age groups, and cannot be interpreted in a unique way. They can reflect crystallization ages or cooling ages. Preservation of titanite ages at 1043-1024 Ma indicates that the exposure at Hensmoen was not reworked or heated above c. 610 °C after 1024 ±9 Ma, and was thus probably exhumed to upper crustal conditions no later than 1024 ±9 Ma.

Orogen-parallel shear zones in the Idefjorden Terrane are interpreted as transpressive thrust zones (Park et al. 1991). To the west of the Oslo Rift, one of these shear zones (an extension of the Ørje Shear Zone) is parallel

to the amphibolite-facies fabric recorded at Hensmoen and presumably coeval with amphibolite-facies metamorphism at c. 1050 Ma (sample B99137, Fig. 5d). So it is reasonable to infer that some of these shear zones were active at c. 1050 Ma. One zircon rim U-Pb date at 974 ±22 Ma in the vicinity of the Göta Älv Shear Zone (Ahlin et al. 2006) nevertheless suggests that the latter was either formed or reactivated at c. 970 Ma in the southern part of the Idefjorden Terrane. Similarly, approaching the Mylonite Zone, zircon U-Pb data record amphibolite-facies metamorphism, migmatitization and associated ductile deformation at 980 ±13 and 971 ±8 Ma (Larson et al. 1999; Andersson et al. 2002; Fig. 10).

Telemarkia Terrane

The four sectors of the Telemarkia Terrane expose rocks from variable paleo-crustal levels. Sveconorwegian metamorphism ranges from low-grade to granulite-facies. Coverage of geochronological data on metamorphism is uneven. Available information nevertheless indicates that the four sectors share a common metamorphic phase in the 1035-1000 Ma interval.

In the low-grade area of central Telemark (Telemark Sector), a mineral Pb-Pb isochron in a 1476 ±13 Ma granite reflects isotopic homogenization at 1031 ±32 Ma, probably related to deformation and metamorphism (Andersen et al. 2002b). In the low-grade area of the Suldal Sector (Sæsvatn-Valdal sequence), a molybdenite Re-Os age of 1032 ±2 Ma defines epidote-amphibolite-facies deformation in a metabasalt (Stein & Bingen 2002; Fig. 10).

Large gneissic areas in the Telemark, Hardangervidda and Suldal Sectors are affected by amphibolite-facies metamorphism. This metamorphism is poorly documented, and has commonly been assumed to be pre-Sveconorwegian, though this assumption has very little support in the geochronological data. On Hardangervidda, a zircon U-Pb date at 1468 ±12 Ma in a migmatitic gneiss possibly defines pre-Sveconorwegian migmatitization (Sigmond et al. 2000). A zircon rim at 1066 ±56 Ma from the same area nevertheless attests to Sveconorwegian amphibolite-facies overprint (Birkeland et al. 1997).

In the northeast of the Telemark Sector, zircon U-Pb data in one sample from the Hallingdal Complex records amphibolite-facies metamorphism at 1014 ±1 Ma (sample B99130, Fig. 7f). In the southeast part of the Telemark Sector (South Telemark Gneisses), the timing of peak amphibolite-facies metamorphism is not directly established, though evidence for metamorphic overprint in 1220-1130 Ma plutons and titanite ages at c. 913 to 901 ±7 Ma implies Sveconorwegian high-grade metamorphism (Heaman & Smalley 1994; Bingen et al. 1998). In the Suldal Sector, a monazite date at 1005 ±7 Ma in a pelitic gneiss (sample B0234, Fig. 8a) reflects amphibolite-facies metamorphism and migmatitization, in accordance with a titanite date at 1009 ±10 Ma in a c. 1035 Ma granite (Andersen et al. 2002a).

The geochronology of high-grade metamorphism in Rogaland-Vest Agder is well documented (Fig. 10). SIMS data on metamorphic zircon from nine samples range from 1068 ±28 to 901 ±18 Ma (Möller et al. 2002; Möller et al. 2003; Tomkins et al. 2005). The data define two modes, a mode between 1030 and 990 Ma related to M1 metamorphism and a mode at 930-920 Ma attributed to M2–M3 metamorphism. A specific zircon population at 955 ±8 Ma has been observed included in cordierite coronas around garnet in a metapelite in the granulite-facies domain (Tomkins et al. 2005). Cordierite coronas are interpreted as a product of a decompression reaction (Jansen et al. 1985; Tomkins et al. 2005) and consequently the 955 ±8 Ma zircons record this regional decompression following M1 metamorphism. The existence of 927 ±7 Ma zircon rims in apparent equilibrium with M2 ultrahigh temperature granulite-facies assemblages links the osumilite and pigeonite isograds to intrusion of the Rogaland AMC complex (Möller et al. 2003).

Monazite SIMS U-Pb data from a granulite, situated outside the area affected by M2 metamorphism (sample B00158, Fig. 8b), provides evidence for two monazite crystallization events at 1032 ±5 and 990 ±8 Ma, the first one probably pertaining to granulite-facies conditions, and both of them related to M1 metamorphism.

Monazite U-Pb ID-TIMS data (Bingen & van Breemen 1998a, this work) define three main age groups (Fig. 11). In the amphibolite facies domain (to the west of the clinopyroxene isograd), the most frequent group ranges from 1012 ±1 to 974 ±2 Ma ($^{207}Pb/^{235}U$ ages) and is attributed to regional M1 metamorphism. The second group, from 930 ±2 to 924 ±2 Ma, is attributed to M2 metamorphism. The third group is restricted to U-poor monazite in hornblende-rich samples. It ranges from 912 ±3 to 904 ±5 Ma, and is attributed to a hydrothermal event. In the granulite-facies domain, the same three groups are evident, except that the first group covers a larger interval from 1024 ±1 to 970 ±5 Ma, and a scatter of dates is detectable between these three main groups. Paired Th-Pb and U-Pb ID-TIMS data in the same sample collection (Fig. 9, Table 4) yield overlapping age groups from 1013 ±5 to 980 ±5 Ma for M1 and from 927 ±5 to 922 ±5 Ma for M2, ($^{208}Pb/^{232}Th$ ages equivalent to $^{207}Pb/^{235}U$ and $^{206}Pb/^{238}U$ ages). A few dates between and after these events are also recorded. The paired Th-U-Pb data confirm an unusually long time span, of at least 33 m.y., for M1 metamorphism (1013-980 Ma), and a tight bracket for M2 metamorphism (927-922 Ma) linking this event to intrusion of the Rogaland AMC plutonism (932 ±3 to 920 ±3 Ma; Schärer et al. 1996). In detail, these data corroborate observations based on U-Pb data (Bingen & van Breemen 1998a; Fig. 11), namely that (1) anhydrous samples collected close to the contact of the AMC complex, west of the pigeonite isograd, paradoxically contain only monazite related to M1 metamorphism (sample B649, 1013-980 Ma), (2) monazite related to M2 metamorphism occurs mainly in the amphibolite-facies domain

between the clinopyroxene and orthopyroxene isograds (samples B135, B185), and (3) monazite crystallization between M1 and M2 metamorphism (930-970 Ma interval) is probably a marginal feature of samples situated in the granulite-facies domain west of the orthopyroxene isograd (sample B191, 947 ±5 Ma).

Available monazite data patterns provide support for four important implications of regional magnitude, namely that (1) M1 regional metamorphism peaked in granulite-facies conditions, (2) M1 metamorphism left charnockitic gneisses in the granulite-facies domain without enough reagent minerals and fluid to crystallize another generation of monazite during M2 metamorphism, (3) the clinopyroxene isograd relates to M2 metamorphism, and (4) the rocks exposed today to the west of the orthopyroxene isograd were probably not exhumed to upper crustal conditions between the M1 and M2 metamorphic events, but probably resided in "reactive" middle crustal conditions.

Molybdenite associated with quartz veins, leucosomes or pegmatite bodies from seven localities yields Re-Os ages ranging from 982 ±3 to 917 ±3 Ma (Bingen & Stein 2003; Bingen et al. 2006). Molybdenite probably crystallized from trace Mo liberated from biotite, magnetite and ilmenite after peak M1 metamorphism. In the Ørsdalen deposit, west of the orthopyroxene isograd, 973 ±4 Ma molybdenite is the product of biotite dehydration melting and is taken as evidence for granulite-facies decompression melting after the peak of M1 metamorphism (Bingen & Stein 2003; Stein 2006; Fig. 10). The molybdenite data were collected from deformed Mo deposits. Consequently, they constrain the last increment of ductile deformation to be younger than 947 ±3 Ma in the amphibolite-facies domain to the east of the clinopyroxene isograd, and younger than 931 ±3 Ma to the west of this isograd (Bingen et al. 2006). A deformation event younger than 917 ±3 Ma is recorded in direct contact to the anorthosite plutons. Molybdenite data suggest that the regional N-S trending structural pattern is largely younger than c. 950 Ma, and imply that intrusion of the anorthosite plutons was associated with ductile deformation, at least up to 10 km away from the plutons. This rules out models featuring M2 metamorphism as a phase of static contact metamorphism controlled only by thermal conductivity (Westphal et al. 2003).

Titanite data in 12 samples from Rogaland-Vest Agder define a regional scale age cluster at 918 ±2 Ma, interpreted as cooling through c. 610 °C (Bingen & van Breemen 1998a; Fig. 10). Amphibole $^{40}Ar/^{39}Ar$ plateau or inverse isochron ages range from 1059 ±8 to 853 ±3 Ma (Bingen et al. 1998). The main age group at 871 ±10 Ma

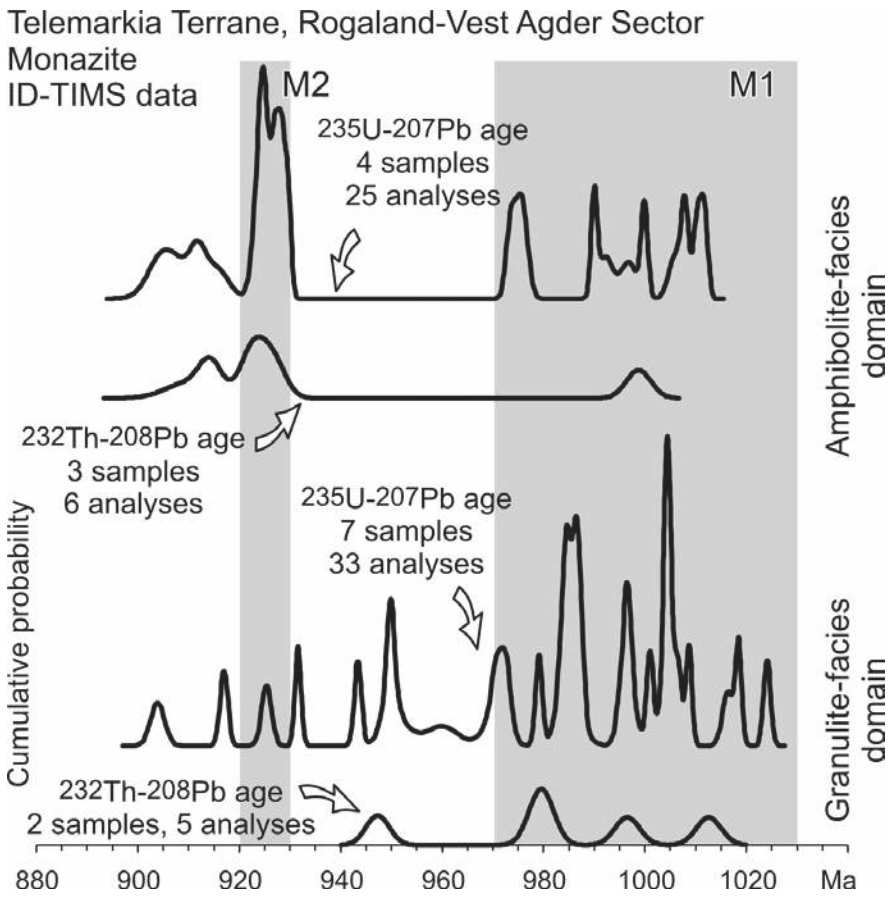

Fig. 11. Cumulative probability diagram with monazite ID-TIMS data in the amphibolite-facies (west of the clinopyroxene isograd) and granulite-facies (west of the orthopyroxene isograd) domains in the Rogaland-Vest Agder Sector. Two curves are presented for each domain, a curve with 207Pb/235U ages and a curve with 208Pb/232Th ages supported by equivalent 207Pb/235U ages (Fig. 9). Data from Bingen and van Breemen (1998a) and Table 4.

is interpreted as a cooling through c. 550-500 °C and overlaps with biotite Rb-Sr ages (Verschure et al. 1980).

Zircon, monazite, titanite and molybdenite geochronology in the Rogaland-Vest Agder Sector (Fig. 10) collectively indicates that this domain was affected by protracted high-grade metamorphism between c. 1035 and 900 Ma, including two main metamorphic events, M1 (1035-970 Ma, intermediate-pressure) and M2 (930-920 Ma, low-pressure, high-temperature). Both peaked in granulite-facies conditions, and both were associated with deformation. The data show that the orthopyroxene isograd is a composite M1-M2 isograd, while the clinopyroxene, osumilite and pigeonite isograds relate to M2. The data record regional decompression between M1 and M2 at 970-955 Ma. M2 metamorphism is a phase of high- to ultrahigh-temperature, low-pressure metamorphism related to intrusion of the Rogaland anorthosites and spatially restricted to the west of the clinopyroxene isograd.

The Vardefjell Shear Zone between the Telemarkia and Idefjorden Terranes (Fig. 1) dips to the southwest, implying that the Telemarkia Terrane is overlying the Idefjorden Terrane along this boundary. The timing of amphibolite-facies metamorphism in rocks affected by deformation along the Vardefjell Shear Zone is estimated at c. 1010 Ma by zircon data in two samples (1012 ±7 Ma for B99111, 1008 ±14 Ma for B99114, Fig. 7b, d). This is consistent with the observation that the Heddal group at the top of the Telemark supracrustal sequence (<1121 ±15 Ma, Bingen et al. 2003) is affected by deformation and metamorphism along the shear zone. Deformation along the Vardefjell Shear Zone is coeval or younger than peak amphibolite-facies conditions at 1010 Ma. Post-peak mylonitization (grain-size reduction) is younger than 1010 Ma. Fabric-parallel titanite may record continued deformation at 985 ±5 Ma. The c. 1010-985 Ma metamorphism in the shear zone (samples B99111-114, Fig. 7) largely overlaps with metamorphism in the Telemarkia hanging wall of the shear zone at 1014 Ma (sample B99130, Fig. 7f), but is younger than metamorphism in the Idefjorden foot wall at 1050-1025 Ma (samples B99137-140-143, Fig. 5). The geometric and geochronologic relations along the Vardefjell Shear Zone allows for a component of northeastwards thrusting at or after 1010 Ma. Nevertheless, they exclude the possibility that metamorphism in the foot wall is a consequence of loading related to thrusting along the shear zone. A significant strike-slip component is possible, in accordance with sinistral strike-slip relations recorded in the Østfold-Marstrand Boundary zone, along strike, and east of the Oslo rift (Hageskov 1985). Additional structural investigations are necessary to establish a tectonic scenario along the Vardefjell Shear Zone. Titanite data (Fig. 7e) suggest that the Vardefjell Shear Zone did not accommodate late orogenic extensional deformation after c. 985 Ma.

Conclusions

The four terranes exposed in the Sveconorwegian belt in south Norway are characterized by distinct Sveconorwegian metamorphic histories (Fig. 10). The Bamble and Kongsberg Terranes bear evidence of an early Sveconorwegian metamorphism between 1140 and 1080 Ma peaking in granulite-facies conditions in the Bamble Terrane at 1140-1125 Ma. These terranes were not significantly overprinted after 1080 Ma by younger metamorphic events recorded in the Telemarkia and Idefjorden Terranes.

The Idefjorden Terrane was possibly affected locally at c. 1090 Ma by this early metamorphism. The main metamorphism took place between c. 1050 and 1025 Ma. This metamorphism generally reached high-pressure, upper amphibolite-facies conditions with pressure-temperature conditions estimated at 1.00-1.17 GPa, 688-780 °C. Coeval high-pressure granulite-facies conditions are locally recorded in the east of the terrane (Söderlund et al. 2008). After c. 1025 Ma, internal and bounding shear zones, namely the Göta Älv Shear Zone and the Mylonite Zone were active under amphibolite-facies conditions at c. 980-970 Ma.

The Telemarkia Terrane was reworked at and after c. 1035 Ma. Amphibolite-facies metamorphism in the Telemark and Suldal sectors peaked between c. 1035 and 1000 Ma. Metamorphism in the Vardefjell Shear Zone between the Telemarkia and Idefjorden Terranes is estimated at c. 1010 Ma, and is coeval with metamorphism in the Telemarkia hanging wall. The Rogaland-Vest Agder Sector was affected by two main metamorphic events peaking in granulite-facies conditions. Medium-pressure, protracted, regional M1 metamorphism took place between 1035 and 970 Ma and was followed by a phase of decompression at 970-955 Ma. Low-pressure high-temperature M2 metamorphism peaked at 930-920 Ma around the Rogaland anorthosite-mangerite-charnockite (AMC) Complex and was related to intrusion of this complex.

Acknowledgements:
Members of the staff at the geochronology laboratory at the Geological Survey of Canada are thanked for help with data acquisition. M. Erambert performed the microprobe analyses. T. Bjerkgård provided sample BU9601 from the Skuterud mine. M. Marker, A. Mulch, E. Sigmond and G. Viola shared field work. U. Söderlund read the manuscript and provided copies of submitted manuscripts. N. Rayner and P. Padget read the manuscript. This paper benefited from constructive reviews by J. Andersson and F. Corfu. This is GSC #20080043

References

Åhäll, K.I., Cornell, D.H. & Armstrong, R. 1998: Ion probe zircon dating of metasedimentary units across the Skagerrak: new constraints for early Mesoproterozoic growth of the Baltic Shield. *Precambrian Research 87*, 117-134.

Åhäll, K.I. & Connelly, J.N. 2008: Long-term convergence along SW Fennoscandia: 330 m.y. of Proterozoic crustal growth. *Precambrian Research 161,* 452-474.

Ahlin, S., Austin Hegardt, E. & Cornell, D. 2006: Nature and stratigraphic position of the 1614 Delsjön augen granite-gneiss in the Median Segment of south-west Sweden. *GFF 128*, 21-32.

Andersen, T. & Munz, I.A. 1995: Radiogenic whole-rock lead in Precambrian metasedimentary gneisses from South Norway: evidence of Sveconorwegian LILE mobility. *Norsk Geologisk Tidsskrift 75,* 156-168.

Andersen, T. & Grorud, H.F. 1998: Age and lead isotope systematics of uranium-enriched cobalt mineralization in the Modum complex, South Norway; implications for Precambrian crustal evolution in the SW part of the Baltic Shield. *Precambrian Research 91*, 419-432.

Andersen, T., Andresen, A. & Sylvester, A.G. 2001: Nature and distribution of deep crustal reservoirs in the southwestern part of the Baltic Shield: evidence from Nd, Sr and Pb isotope data on late Sveconorwegian granites. *Journal of the Geological Society, London 158*, 253-267.

Andersen, T., Andresen, A. & Sylvester, A.G. 2002a: Timing of late- to post-tectonic Sveconorwegian granitic magmatism in South Norway. *Norges geologiske undersøkelse Bulletin 440*, 5-18.

Andersen, T., Sylvester, A.G. & Andresen, A. 2002b: Age and petrogenesis of the Tinn granite, Telemark, South Norway, and its geochemical relationship to metarhyolite of the Rjukan group. *Norges geologiske undersøkelse Bulletin 440*, 19-26.

Andersen, T., Griffin, W.L., Jackson, S.E., Knudsen, T.L. & Pearson, N.J. 2004a: Mid-Proterozoic magmatic arc evolution at the southwest margin of the Baltic shield. *Lithos 73,* 289-318.

Andersen, T., Laajoki, K. & Saeed, A. 2004b: Age, provenance and tectonostratigraphic status of the Mesoproterozoic Blefjell quartzite, Telemark sector, southern Norway. *Precambrian Research 135*, 217-244.

Andersen, T., Griffin, W.L. & Sylvester, A.G. 2007: Sveconorwegian crustal underplating in southwestern Fennoscandia: LAM-ICPMS U-Pb and Lu-Hf isotope evidence from granites and gneisses in Telemark, southern Norway. *Lithos 93,* 273-287.

Andersson, J., Möller, C. & Johansson, L. 2002: Zircon chronology of migmatite gneisses along the Mylonite Zone (S Sweden): a major Sveconorwegian terrane boundary in the Baltic Shield. *Precambrian Research 114,* 121-147.

Austin Hegardt, E., Cornell, D.H., Hellström, F.A. & Lundqvist, I. 2007: Emplacement age of the mid-Proterozoic Kungsbacka Bimodal Suite, SW Sweden. *GFF 129*, 227-234.

Berthelsen, A. 1980: Towards a palinspastic tectonic analysis of the Baltic Shield. In Cogne, J. & Slansky, M. (eds.), *Geology of Europe, from Precambrian to the post-Hercyninan sedimentary basins, 108*, 5-21. Mémoires du B.R.G.M., Paris.

Bingen, B., Demaiffe, D. & Hertogen, J. 1996: Redistribution of rare-earth elements, Th and U over accessory minerals in the course of amphibolite to granulite facies metamorphism: the role of apatite and monazite in orthogneisses from SW Norway. *Geochimica et Cosmochimica Acta 60*, 1341-1354.

Bingen, B., Boven, A., Punzalan, L., Wijbrans, J. & Demaiffe, D. 1998: Hornblende $^{40}Ar/^{39}Ar$ geochronology across terrane boundaries in the Sveconorwegian province of S Norway. *Precambrian Research 90*, 159-185.

Bingen, B. & van Breemen, O. 1998a: U–Pb monazite ages in amphibolite- to granulite-facies orthogneisses reflect hydrous mineral breakdown reactions: Sveconorwegian Province of SW Norway. *Contributions to Mineralogy and Petrology 132*, 336-353.

Bingen, B. & van Breemen, O. 1998b: Tectonic regimes and terrane boundaries in the high-grade Sveconorwegian belt of SW Norway, inferred from U–Pb zircon geochronology and geochemical signature of augen gneiss suites. *Journal of the Geological Society, London 155*, 143-154.

Bingen, B., Austrheim, H. & Whitehouse, M.J. 2001a: Ilmenite as a source for zirconium during high-grade metamorphism? Textural evidence from the Caledonides of W. Norway and implications for zircon geochronology. *Journal of Petrology 42*, 355-375.

Bingen, B., Birkeland, A., Nordgulen, Ø. & Sigmond, E.M.O. 2001b: Correlation of supracrustal sequences and origin of terranes in the Sveconorwegian orogen of SW Scandinavia: SIMS data on zircon in clastic metasediments. *Precambrian Research 108*, 293-318.

Bingen, B., Mansfeld, J., Sigmond, E.M.O. & Stein, H.J. 2002: Baltica-Laurentia link during the Mesoproterozoic: 1.27 Ga development of continental basins in the Sveconorwegian Orogen, southern Norway. *Canadian Journal of Earth Sciences 39*, 1425-1440.

Bingen, B., Nordgulen, Ø., Sigmond, E.M.O., Tucker, R.D., Mansfeld, J. & Högdahl, K. 2003: Relations between 1.19-1.13 Ga continental magmatism, sedimentation and metamorphism, Sveconorwegian province, S Norway. *Precambrian Research 124,* 215-241.

Bingen, B. & Stein, H.J. 2003: Molybdenite Re-Os dating of biotite dehydration melting in the Rogaland high-temperature granulites, S Norway. *Earth and Planetary Science Letters 208*, 181-195.

Bingen, B., Skår, Ø., Marker, M., Sigmond, E.M.O., Nordgulen, Ø., Ragnhildstveit, J., Mansfeld, J., Tucker, R.D. & Liégeois, J.P. 2005: Timing of continental building in the Sveconorwegian orogen, SW Scandinavia. *Norwegian Journal of Geology 85*, 87-116.

Bingen, B., Stein, H.J., Bogaerts, M., Bolle, O. & Mansfeld, J. 2006: Molybdenite Re-Os dating constrains gravitational collapse of the Sveconorwegian orogen, SW Scandinavia. *Lithos 87*, 328-346.

Bingen, B., Nordgulen, Ø. & Viola, G. 2008: A four-phase model for the Sveconorwegian orogeny, SW Scandinavia: *Norwegian Journal of Geology 88,* 43-72.

Birkeland, A., Sigmond, E.M.O., Whitehouse, M.J. & Vestin, J. 1997: From Archaean to Proterozoic on Hardangervidda, South Norway. *Norges geologiske undersøkelse Bulletin 433*, 4-5.

Bogaerts, M., Scaillet, B., Liégeois, J.P. & Vander Auwera, J. 2003: Petrology and geochemistry of the Lyngdal granodiorite (Southern Norway) and the role of fractional crystallization in the genesis of Proterozoic ferro-potassic A-type granites. *Precambrian Research 124*, 149-184.

Bolle, O., Demaiffe, D. & Duchesne, J.C. 2003: Petrogenesis of jotunitic and acidic members of an AMC suite (Rogaland anorthosite province, SW Norway): a Sr and Nd isotopic assessment. *Precambrian Research 124*, 185-214.

Brewer, T.S., Daly, J.S. & Åhäll, K.I. 1998: Contrasting magmatic arcs in the Palaeoproterozoic of the south-western Baltic Shield. *Precambrian Research 92*, 297-315.

Bussy, F., Krogh, T.E., Klemens, W.P. & Schwerdtner, W.M. 1995: Tectonic and metamorphic events in the westernmost Grenville Province, central Ontario: new results from high-precision U–Pb geochronology. *Canadian Journal of Earth Sciences 32*, 660-671.

Cherniak, D.J. 1993: Lead diffusion in titanite and preliminary results on the effects of radiation damage on Pb transport. *Chemical Geology 110*, 177-194.

Cherniak, D.J., Watson, E.B., Grove, M. & Harrison, T.M. 2004: Pb diffusion in monazite: a combined RBS/SIMS study. *Geochimica et Cosmochimica Acta 68*, 829-840.

Cocherie, A., Legendre, O., Peucat, J.J. & Kouamelan, A.N. 1998: Geochronology of polygenetic monazites constrained by in situ electron microprobe Th-U-total Pb determination: implications for Pb behaviour in monazite. *Geochimica et Cosmochimica Acta 62*, 2475-2497.

Connelly, J.N. & Åhäll, K.I. 1996: The Mesoproterozoic cratonization of Baltica – new age constraints from SW Sweden. *In* Brewer, T.S. (ed.), *Precambrian crustal evolution in the North Atlantic Region*.

Geological Society, London, Special Publications, 112, 261-273.
Cosca, M.A. & O'Nions, R.K. 1994: A re-examination of the influence of composition on argon retentivity in metamorphic calcic amphiboles. *Chemical Geology 112*, 39-56.
Cosca, M.A., Mezger, K. & Essene, E.J. 1998: The Baltica-Laurentia connection: Sveconorwegian (Grenvillian) metamorphism, cooling, and unroofing in the Bamble Sector, Norway. *The Journal of Geology 106*, 539-552.
Davis, W.J., McNicoll, V.J., Bellerive, D.R., Santowski, K. & Scott, D.J. 1997: Modified chemical procedures for the extraction and purification of uranium from titanite, allanite, and rutile in the Geochronology Laboratory, Geological Survey of Canada. *Radiogenic age and isotopic studies: report 10; Geological Survey of Canada, Current research 1997-F,* 33-35.
Davis, W.J., Parrish, R.R., McNicoll, V. & Bellerive, D. 1998: Analytical techniques for the determination of 208Pb/232Th ages of monazite and zircon at the Geochronology Laboratory, Geological Survey of Canada. *Radiogenic age and isotopic studies: report 11; Geological Survey of Canada, current research 1998-F,* 19-22.
de Haas, G.J.L.M., Nijland, T.G., Andersen, T. & Corfu, F. 2002: New constraints on the timing of deposition and metamorphism in the Bamble sector, south Norway: zircon and titanite U-Pb data data from the Nelaug area. *GFF 124*, 73-78.
Demaiffe, D. & Michot, J. 1985: Isotope geochronology of the Proterozoic crustal segment of southern Norway: a review. *In* Tobi, A.C. & Touret, J.L. (eds.), *The deep Proterozoic crust in the north Atlantic provinces, NATO-ASI C158,* 411-433. Reidel, Dordrecht.
Dons, J.A. 1960: The stratigraphy of supracrustal rocks, granitization and tectonics in the Precambrian Telemark area, southern Norway. *Norges geologiske undersøkelse 212h*, 1-30.
Falkum, T. 1985: Geotectonic evolution of southern Scandinavia in light of a late-Proterozoic plate-collision. *In* Tobi, A.C. & Touret, J.L. (eds.), *The deep Proterozoic crust in the north Atlantic provinces, NATO-ASI C158*, 309-322. Reidel, Dordrecht.
Fraser, G., Ellis, D. & Eggins, S. 1997: Zirconium abundance in granulite-facies minerals, with implications for zircon geochronology in high-grade rocks. *Geology 25*, 607-610.
Gibson, H.D., Carr, S.D., Brown, R.L. & Hamilton, M.A. 2004: Correlations between chemical and age domains in monazite, and metamorphic reactions involving major pelitic phases: an integration of ID-TIMS and SHRIMP geochronology with U-Th-U X-ray mapping. *Chemical Geology 211*, 237-260.
Grorud, H.F. 1997: Textural and compositional characteristics of cobalt ores from the Skuterud Mines of Modum, Norway. *Norsk Geologisk Tidsskrift 77*, 31-38.
Hageskov, B. 1985: Constrictional deformation of the Koster dyke swarm in a ductile sinistral shear zone, Koster islands, SW Sweden. *Bulletin of the Geological Society of Denmark 34*, 151-197.
Hansen, B.T., Persson, P.O., Söllner, F. & Lindh, A. 1989: The influence of recent lead loss on the interpretation of disturbed U–Pb systems in zircons from metamorphic rocks in southwest Sweden. Lithos 23, 123-136.
Harlov, D.E. 2000: Pressure-temperature estimation in orthopyroxene-garnet bearing granulite facies rocks, Bamble Sector, Norway. *Mineralogy and Petrology 69*, 11-33.
Heaman, L.M. & Smalley, P.C. 1994: A U–Pb study of the Morkheia Complex and associated gneisses, south Norway: implications for disturbed Rb–Sr systems and for the temporal evolution of Mesoproterozoic magmatism in Laurentia. *Geochimica et Cosmochimica Acta 58*, 1899-1911.
Hellström, F.A., Johansson, Å. & Larson, S.Å. 2004: Age emplacement of late Sveconorwegian monzogabbroic dykes, SW Sweden. *Precambrian Research 128*, 39-55.
Henderson, I.H.C. & Ihlen, P.M. 2004: Emplacement of polygeneration pegmatites in relation to Sveconorwegian contractional tectonics: examples from southern Norway. *Precambrian Research 133,* 207-222.
Holland, T.J., Babu, E.V. & Waters, D.J. 1996: Phase relations of osumilite and dehydration melting in pelitic rocks: a simple thermodynamic model for the KFMASH system. *Contributions to Mineralogy and Petrology 124*, 383-394.
Holland, T.J.B. & Powell, R. 1998: An internally consistent thermodynamic data set for phases of petrological interest. *Journal of Metamorphic Geology 16,* 309-343.
Jansen, J.B.H., Blok, R.J., Bos, A. & Scheelings, M. 1985: Geothermometry and geobarometry in Rogaland and preliminary results from the Bamble area, S Norway. *In* Tobi, A.C. & Touret, J.L. (eds.), *The deep Proterozoic crust in the north Atlantic provinces, NATO-ASI C158*, 499-516. Reidel, Dordrecht.
Johansson, L., Lindh, A. & Möller, C. 1991: Late Sveconorwegian (Grenville) high-pressure granulite facies metamorphism in southwest Sweden. *Journal of Metamorphic Geology 9*, 283-292.
Johansson, L., Möller, C. & Söderlund, U. 2001: Geochronology of eclogite facies metamorphism in the Sveconorwegian Province of SW Sweden. *Precambrian Research 106*, 261-275.
Kaneko, Y. & Miyano, T. 2004: Recalibration of mutually consistent garnet-biotite and garnet-cordierite geothermometers. *Lithos 73,* 255-269.
Knudsen, T.L., Andersen, T., Maijer, C. & Verschure, R.H. 1997a: Trace-element characteristics and Pb isotopic evolution of metasediments and associated Proterozoic rocks from the amphibolite- to granulite-facies Bamble sector, southern Norway. *Chemical Geology 143*, 145-169.
Knudsen, T.L., Andersen, T., Whitehouse, M.J. & Vestin, J. 1997b: Detrital zircon ages from southern Norway - implications for the Proterozoic evolution of the southwestern Baltic Shield. *Contributions to Mineralogy and Petrology 130,* 47-58.
Knudsen, T.L. & Andersen, T. 1999: Petrology and geochemistry of the Tromøy gneiss complex, South Norway, an alleged example of Proterozoic depleted lower continental crust. *Journal of Petrology 40,* 909-933.
Krogh, E.J., Andresen, A., Bryhni, I., Broks, T.M. & Kristensen, S.E. 1990: Eclogites and polyphase P-T cycling in the Uppermost Allochton in Troms, northern Norway. *Journal of Metamorphic Geology 8,* 289-309.
Kullerud, L. & Dahlgren, S.H. 1993: Sm-Nd geochronology of Sveconorwegian granulite facies mineral assemblages in the Bamble shear belt, south Norway. *Precambrian Research 64*, 389-402.
Laajoki, K., Corfu, F. & Andersen, T. 2002: Lithostratigraphy and U-Pb geochronology of the Telemark supracrustals in the Bandak-Sauland area, Telemark, South Norway. *Norwegian Journal of Geology 82,* 119-138.
Larson, S.Å., Cornell, D.H. & Armstrong, R.A. 1999: Emplacement ages and metamorphic overprinting of granitoids in the Sveconorwegian Province in Värmland, Sweden - an ion probe study. *Norsk Geologisk Tidsskrift 79*, 87-96.
Lindh, A., Gorbatschev, R. & Lundegårdh, P.H. 1998: Beskrivning till berggrundskartan över Värmland Län; Västra Värmlands Berggrund. *Sveriges Geologiska Undersökning Ser. Ba, 45:2*, 1-405.
Ludwig, K.R. 1998: On the treatment of concordant uranium-lead ages. *Geochimica et Cosmochimica Acta 62*, 665-676.
Ludwig, K.R. 2001: Users manual for Isoplot/Ex version 2.49, a geochronological toolkit for Microsoft Excel. Berkeley Geochronology Center, Special Pubication No. 1a, Berkley.
Lundqvist, I. & Skiöld, T. 1993: U-Pb zircon dating of volcanic rocks of the Åmål Group, western Sweden. *In* Lundqvist, T. (ed.), *Radiometric dating results, C823*, 24-30. Sveriges Geologiska Undersökning, Uppsala.
Möller, A., O'Brien, P.J., Kennedy, A. & Kröner, A. 2002: Polyphase zircon in ultrahigh-temperature granulites (Rogaland, SW Norway): constraints for Pb diffusion in zircon. *Journal of Metamorphic Geology 20*, 727-740.
Möller, A., O'Brien, P.J., Kennedy, A. & Kröner, A. 2003: Linking growth episodes of zircon and metamorphic textures to zircon chemistry:

an example from the ultrahigh-temperature granulites of Rogaland (SW Norway). *In* Vance, D., Müller, W. & Villa, I.M. (eds.), *Geochronology: linking the isotopic record with petrology and textures.* Geological Society, London, Special Publications, *220*, 65-81.

Morton, R.D. 1971: Geological investigations in the Bamble sector of the Fennoscandian Shield, S. Norway. No II. Metasediments and metapyroclastics (?) within the Precambrian metamorphic suite of the S Norwegian Skaergaard. *Norsk Geologisk Tidsskrift 51*, 63-83.

Mulch, A., Cosca, M.A., Andresen, A. & Fiebig, J. 2005: Time scales of deformation and exhumation in extensional detachment systems determined by high-spatial resolution in situ UV-laser 40Ar/39Ar dating. *Earth and Planetary Science Letters 233*, 375-390.

Munz, I.A. 1990: Whiteschists and orthoamphibole-cordierite rocks and the P-T-t path of the Modum Complex, South Norway. *Lithos 24*, 181-200.

Munz, I.A., Wayne, D. & Austrheim, H. 1994: Retrograde fluid infiltration in the high-grade Modum Complex, S Norway: evidence for age, source and REE mobility. *Contributions to Mineralogy and Petrology 116*, 32-46.

Nijland, T.G. & Maijer, C. 1993: The regional amphibolite to granulite facies transition at Arendal, Norway: evidence for a thermal dome. *Neues Jahrbuch für Mineralogie, Abhandlungen 165,* 191-221.

Nijland, T.G., Maijer, C., Senior, A. & Verschure, R.H. 1993: Primary sedimentary structures and compositions of the high-grade metamorphic Nidelva Quartzite Complex (Bamble, Norway), and the origin of nodular gneisses. *Proceedings Koninklijke Nederlandse Akademie van Wetenschappen 96,* 217-232.

Park, R.G., Åhäll, K.I. & Boland, M.P. 1991: The Sveconorwegian shear-zone network of SW Sweden in relation to mid-Proterozoic plate movements. *Precambrian Research 49*, 245-260.

Parrish, R.R., Roddick, J.C., Loveridge, W.D. & Sullivan, R.W. 1987: Uranium-lead analytical techniques at the geochronology laboratory, Geological Survey of Canada. *Radiogenic age and isotopic studies, report 1; Geological Survey of Canada, Current Research 87-2*, 3-7.

Pasteels, P. & Michot, J. 1975: Geochronologic investigation of the metamorphic terrain of southwestern Norway. *Norsk Geologisk Tidsskrift 55*, 111-134.

Perchuk, L.L., Aranovich, L., Podlesskiy, K.K., Lavrantyeva, I.V., Gerasimov, V.Y., Fedkin, V.V., Kitsul, V.I., Karsakov, L.P. & Berdnikov, N.V. 1985: Precambrian granulites of the Aldan shield, eastern Siberia, USSR. *Journal of Metamorphic Petrology 3*, 265-310.

Pyle, J.M. & Spear, F.S. 2003: Four generations of accessory-phase growth in low-pressure migmatites from SW New Hampshire. *American Mineralogist 88*, 338-351.

Schärer, U. 1984: The effect of initial ^{230}Th disequilibrium on young U-Pb ages: the Makalu case, Himalaya. *Earth and Planetary Science Letters 67*, 191-204.

Schärer, U., Wilmart, E. & Duchesne, J.C. 1996: The short duration and anorogenic character of anorthosite magmatism: U-Pb dating of the Rogaland complex, Norway. *Earth and Planetary Science Letters 139*, 335-350.

Sigmond, E.M.O. 1978: Beskrivelse til det berggrunnsgeologiske kartbladet Sauda 1:250000. *Norges geologiske undersøkelse Bulletin 341*, 1-94.

Sigmond, E.M.O. 1998: Geologisk kart over Norge, berggrunnskart Odda, 1:250000. Norges geologiske undersøkelse, Trondheim.

Sigmond, E.M.O., Birkeland, A. & Bingen, B. 2000: A possible basement to the Mesoproterozoic quartzites on Hardangervidda, South-central Norway: zircon U-Pb geochronology of a migmatitic gneiss. *Norges geologiske undersøkelse Bulletin 437*, 25-32.

Smalley, P.C., Field, D., Lamb, R.C. & Clough, P.W.L. 1983: Rare earth, Th, Hf, Ta, and large-ion lithophile element variations in metabasites from the Proterozoic amphibolite-granulite transition zone at Arendal, South Norway. *Earth and Planetary Science Letters 63*, 446-458.

Smith, H.A. & Barreiro, B. 1990: Monazite U-Pb dating of staurolite grade metamorphism in pelitic schists. *Contributions to Mineralogy and Petrology 105*, 602-615.

Smoliar, M.I., Walker, R.J. & Morgan, J.W. 1996: Re-Os isotope constraints on the age of Group IIA, IIIA, IVA, and IVB iron meteorites. *Science 271*, 1099-1102.

Söderlund, U., Jarl, L.G., Persson, P.O., Stephens, M.B. & Wahlgren, C.H. 1999: Protolith ages and timing of deformation in the eastern, marginal part of the Sveconorwegian orogen, southwestern Sweden. *Precambrian Research 94*, 29-48.

Söderlund, U., Hellström, F.A. & Kamo, S.L. 2008: Geochronology of high-pressure mafic granulite dykes in SW Sweden; tracking the P-T-t path of metamorphism using Hf isotopes in zircon and baddeleyite. *Journal of Metamorphic Geology (in press)*.

Stacey, J.S. & Kramers, J.D. 1975: Approximation of terrestrial lead isotope evolution by a two-stage model. *Earth and Planetary Science Letters 26*, 207-221.

Starmer, I.C. 1985: The evolution of the south Norwegian Proterozoic as revealed by the major and mega-tectonics of the Kongsberg and Bamble sector. In Tobi, A.C. & Touret, J.L. (eds.), *The deep Proterozoic crust in the north Altantic provinces, NATO-ASI C158,* 259-290. Reidel, Dordrecht.

Starmer, I.C. 1991: The Proterozoic evolution of the Bamble sector shear belt, southern Norway: correlations across southern Scandinavia and the Grenvillian controversy. *Precambrian Research 49*, 107-139.

Stein, H.J., Markey, R.J., Morgan, J.W., Hannah, J.L. & Scherstén, A. 2001: The remarkable Re-Os chronometer in molybdenite: how and why it works. *Terra Nova 13*, 479-486.

Stein, H.J. & Bingen, B. 2002: 1.05-1.01 Ga Sveconorwegian metamorphism and deformation of the supracrustal sequence at Sæsvatn, South Norway: Re-Os dating of Cu-Mo mineral occurrences. *In* Blundell, D., Neubauer, F. & von Quadt, A. (eds.), *The timing and location of major ore deposits in an evolving orogen.* Geological Society, London, Special Publications, 204, 319-335.

Stein, H.J. 2006: Low-rhenium molybdenite by metamorphism in northern Sweden: recognition, genesis, and global implications. *Lithos 87*, 300-327.

Stern, R.A. 1997: The GSC Sensitive High Resolution Ion Microprobe (SHRIMP): analytical techniques of zircon U-Th-Pb age determination and performance evaluation. *Radiogenic Age and Isotopic Studies, report 10; Geological Survey of Canada, Current Research 97-F*, 1-31.

Stern, R.A. & Berman, R.G. 2000: Monazite U–Pb and Th–Pb geochronology by ion microprobe, with application to in situ dating of an Archean metasedimentary rock. *Chemical Geology 172*, 113-130.

Stern, R.A. & Amelin, Y. 2003: Assessment of errors in SIMS zircon U-Pb geochronology using a natural zircon standard and NIST SRM 610 glass. *Chemical Geology 197*, 111-142.

Tobi, A.C., Hermans, G.A., Maijer, C. & Jansen, J.B.H. 1985: Metamorphic zoning in the high-grade Proterozoic of Rogaland-Vest Agder, SW Norway. *In* Tobi, A.C. & Touret, J.L. (eds.), *The deep Proterozoic crust in the north Atlantic provinces, NATO-ASI C158,* 477-497. Reidel, Dordrecht.

Tomkins, H.S., Williams, I.S. & Ellis, D.J. 2005: In situ U-Pb dating of zircon formed from retrograde garnet breakdown during decompression in Rogaland, SW Norway. *Journal of Metamorphic Geology 23*, 201-215.

Touret, J.L. 1971: Le facies granulite en Norvège méridionale. 1. Les associations minéralogiques. *Lithos 4*, 239-249.

Vander Auwera, J. 1993: Diffusion controlled growth of pyroxene-bearing margins on amphibolite bands in the granulite facies of Rogaland (southwestern Norway): implications for granulite formation. *Contributions to Mineralogy and Petrology 114,* 203-220.

Vander Auwera, J., Bogaerts, M., Liégeois, J.P., Demaiffe, D., Wilmart, E., Bolle, O. & Duchesne, J.-C. 2003: Derivation of the 1.0–0.9 Ga ferro-potassic A-type granitoids of southern Norway by extreme

differentiation from basic magmas. *Precambrian Research 124*, 107-148.

Verschure, R.H., Andriessen, P.A.M., Boelrijk, N.A.M., Hebeda, E.H., Maijer, C., Priem, H.N.A. & Verdurmen, E.A.T. 1980: On the thermal stability of Rb-Sr and K-Ar biotite systems: evidence from coexisting Sveconorwegian (ca 870 Ma) and (ca 400 Ma) biotites in SW Norway. *Contributions to Mineralogy and Petrology 74*, 245-252.

Visser, D. & Senior, A. 1990: Aluminous reaction textures in ortho-amphibole-bearing rocks: the pressure-temperature evolution of the high-grade Proterozoic of the Bamble sector, south Norway. *Journal of Metamorphic Geology 8*, 231-246.

Westphal, M., Schumacher, J.C. & Boschert, S. 2003: High-temperature metamorphism and the role of magmatic heat sources at the Rogaland Anorthosite Complex in Southwestern Norway. J*ournal of Petrology 44*, 1145-1162.

Williams, I.S. 2001: Response of detrital zircon and monazite, and their U-Pb isotopic systems, to regional metamorphism and host-rock partial melting, Cooma complex, southeastern Australia. *Australian Journal of Earth Sciences 48*, 557-580.

Williams, M.L., Jercinovic, M.J. & Hetherington, C.J. 2007: Microprobe monazite geochronology: Understanding geologic processes by integrating composition and chronology. *Annual Review of Earth and Planetary Sciences 35*, 137-175.